Chapter 8

Excavations At DgRw 199-F 1

The existence of a burial cave at DgRw 199 has long been known to local residents and visitors to Gabriola Island, but it was not until 1987 that the cave was formally recorded as an archaeological site, during a systematic reconnaissance of the False Narrows bluffs (Wilson 1987). Wilson described three separate burial areas at DgRw 199, the largest of which [Feature 1] contained the remains of a minimum of seven individuals, based on the number of skulls visible. Differential preservation of these skulls led Wilson to conclude that the burials had been deposited on the surface, and represented more than one interment event. He also observed evidence of disturbance from both animal scavenging and human vandalism, including a small hand screen and spoon which had presumably been used to sift the cave sediments for artifacts.

Later that year a burial recovery project was initiated to collect all cultural material visible on the surface of the cave, and if possible to determine the nature of the site (Skinner 1991). The surface collection was augmented by small-scale test excavations in two locations, which established the presence of shallow subsurface cultural deposits. A minimum of 17 individuals were represented in the skeletal material collected at this time. Skinner suggested that the burials at 199-F1 were probably secondary interments that had been removed from their original burial context and placed in the cave in recent (though pre-Contact) times.

Unfortunately, Skinner's removal of all surface cultural material from the cave did not have the desired effect of discouraging pothunting at the site. Evidence of continued disturbance was a prime factor in the selection of this feature for excavation in 1992. The existence of the earlier skeletal collection was also an important consideration, given the expressed wishes of the Nanaimo First Nation that all of the human remains from a burial site be kept together.

Feature Description

Feature 1, the largest of the burial features discovered in the study area, is located on the lower False Narrows bluffs, at the eastern end of the DgRw 199, about 100 m west of the petroglyph site DgRw 198. Situated near the base of a steep, boulder-strewn, forested slope, in a dense cluster of 11 burial features (Figures 8.1, 8.2), it is fashioned from two massive sandstone blocks which form the ceiling/south wall, and a number of smaller but still substantial sandstone and conglomerate boulders that contribute primarily to the north wall. Beneath the two ceiling slabs is a long, narrow cave-like recess that is constricted near the middle to form two chambers (Figure 8.2). The west chamber is 2.10 m wide, 3.30 m long, and 1.30 m high (maximum dimensions); the east chamber is 2.29 m wide, 3.05 m long, and 0.95 m high (Figures 8.3, 8.4). North of the two principal chambers the jumble of boulders forming the north wall has created numerous small crevices, chimneys (Skinner's "fissure"), and ledges (Skinner's "Upper Gallery") in which human remains were also found. Bats were observed roosting in the Upper Gallery during the 1989 survey.

Access to 199-F1 is via a narrow, low-ceilinged, steeply-sloping, 3-m-long passage located at the west end of the burial feature; this entrance faces roughly northwest. Entry can also be gained (with some difficulty) from the west by climbing over a jumble of boulders and down through the "Upper Gallery". A crack at the east end of the feature was enlarged by Skinner to form a secondary entrance in

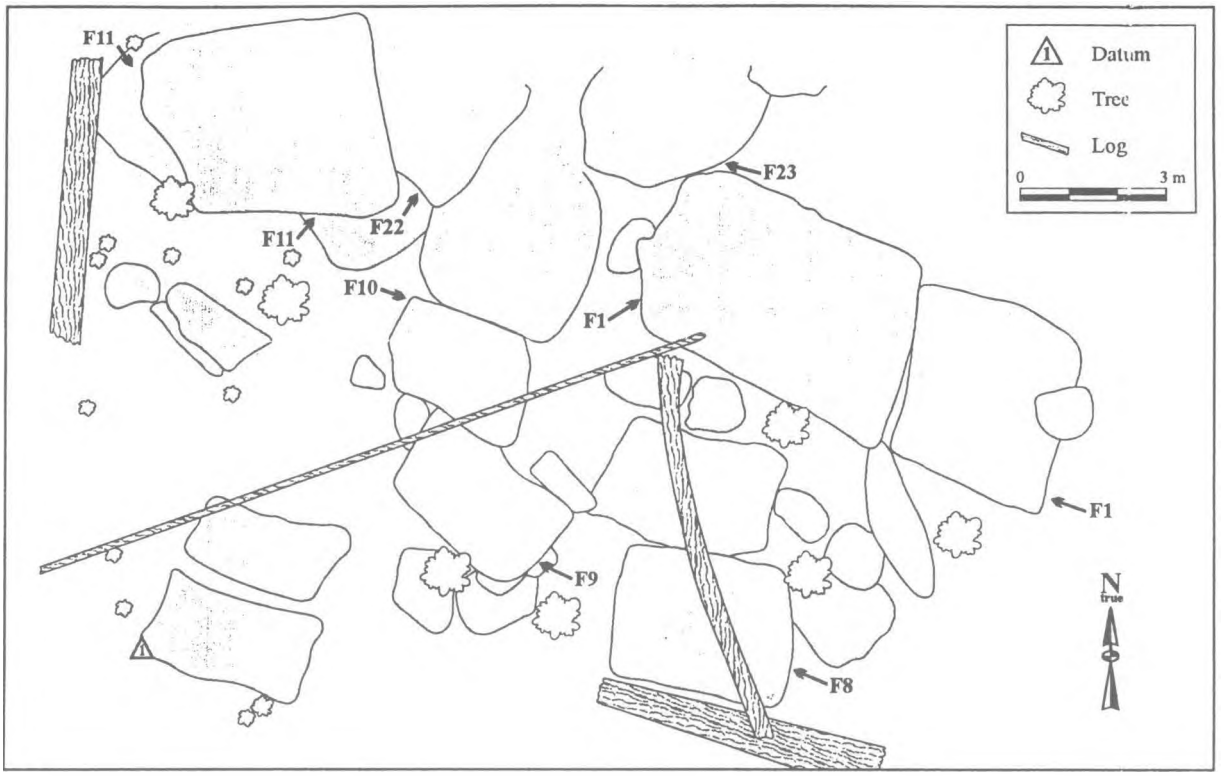

Figure 8.1 DgRw 199-F1 location.

1987, and may have been used as such prehistorically before filling in with sediments; this opening faces almost due south. Another gap between the two ceiling slabs admits some light to the middle of the cave, but is too narrow to allow entry.

Despite the 1987 surface-collection, when 199-F1 was reexamined two years later, more than 100 human bone fragments were visible on the surface, attesting to the degree of continued disturbance to the feature. In the course of the 1989 site survey, several persons were observed visiting the cave site, and there was some evidence of ritual use of the feature by non-Natives on two occasions, on the autumn and spring solstices. Some of the observed disturbance may also have resulted from animal activity, as carnivore faeces were observed in the main cave area.

Excavation Results

A grid of fifteen 1.0 x 1.0 excavation units (EUs) was laid out on the floor of the cave (Figure 8.3), using the east-west baseline established by Skinner in 1987 so that proveniences of the second skeletal collection would be consistent with the first. A natural stone cist located to the north of the main entrance passage was designated EU 16; it also measured approximately 1.0 x 1.0 m. Small unit extensions (EXs) of variable size were excavated to the north of EUs 2, 6, and 15, and to the south of EUs 1, 4, and 13 to complete coverage of the entire floor. All EUs and EXs were excavated in 5-cm arbitrary levels except EU 15, which was dug in natural strata subdivided into 5-cm arbitrary levels.

The entire cave floor, with the exception of EUs 15 and 16, was excavated to culturally sterile deposits (often bedrock or immovable boulders), encountered at 10-40 cm below surface in the east chamber, and 20-60 cm below surface in the west chamber. The bottom levels of EU 16, a deep, well-like stone cist, were inaccessible to the excavator, and although all visible human remains were removed it is possible that additional buried skeletal material is present in this unit. EU 15, located in the west entrance passage, presented an excavation challenge due to the steeply sloping surface and the presence of large unstable boulders that were loosened by removal of the surrounding sediments; as much of this unit was excavated as was consistent with the safety of the excavation crew, but again, some human remains may still be present in this portion of the site. Slumping of loosened sediments also occurred in the lower levels of excavation in EUs 8, 10, 11, and 12, resulting in loss of vertical provenience of materials collected from some quadrants.

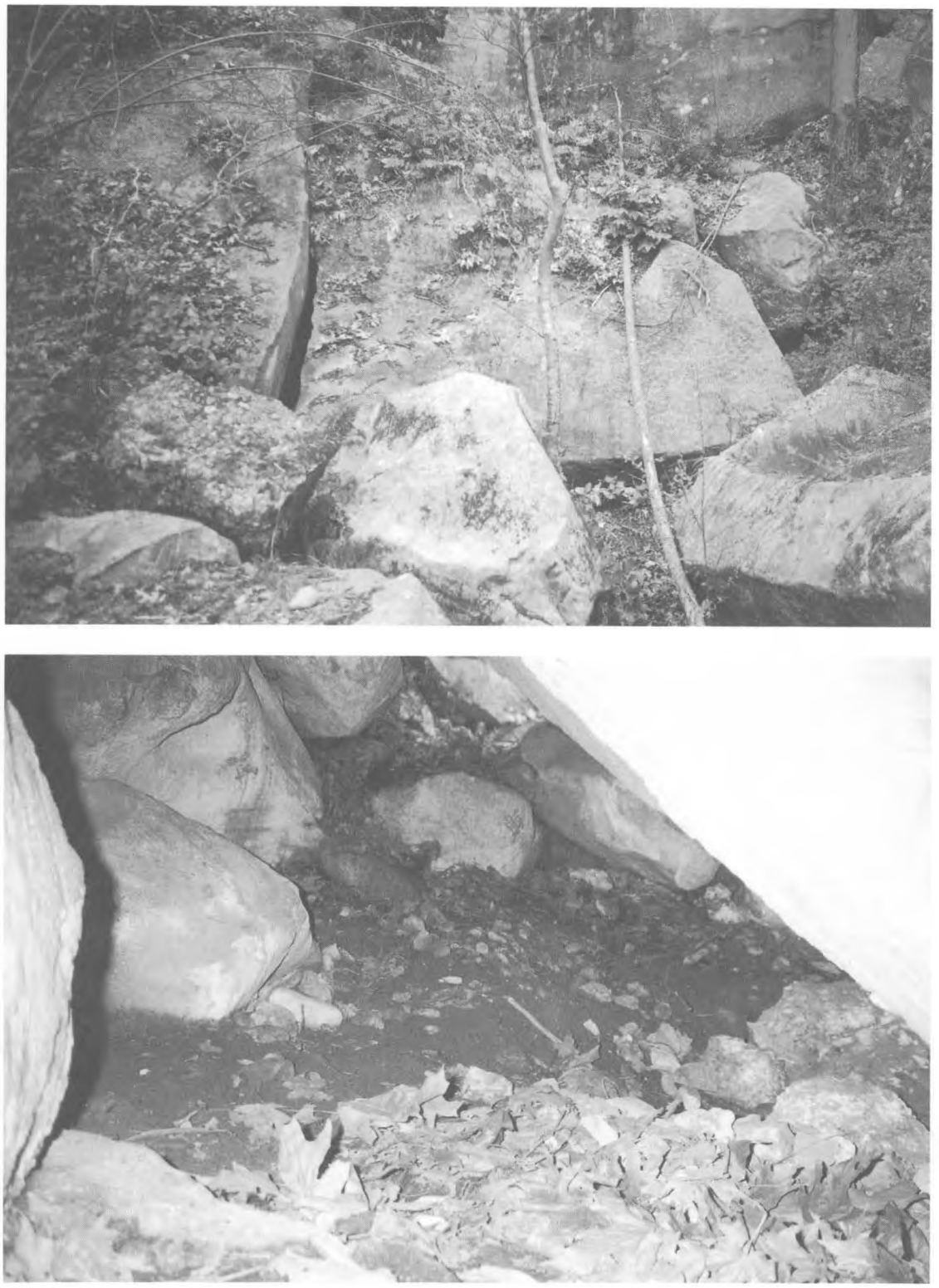

Figure 8.2 View of DgRw 199-F1 from south (top); view inside east chamber, looking east (bottom).

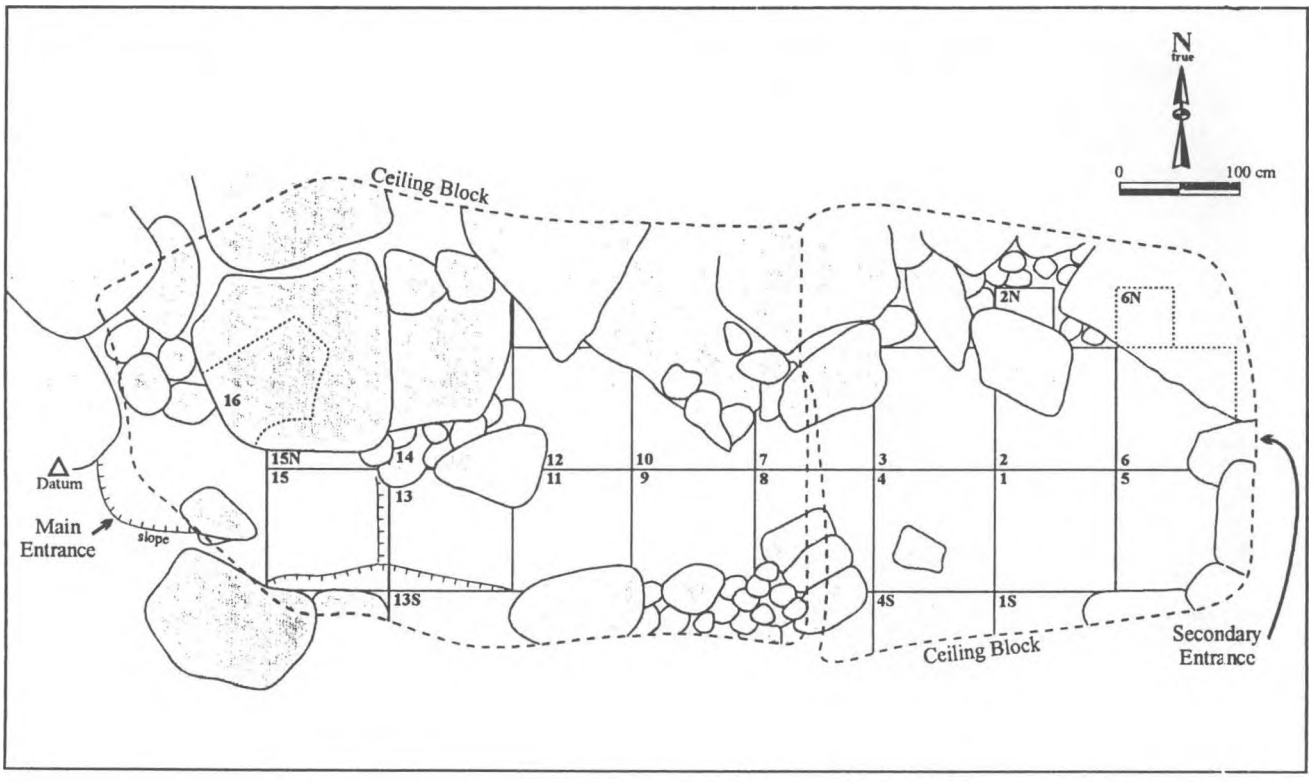

Figure 8.3 DgRw 199-F1: floor plan.

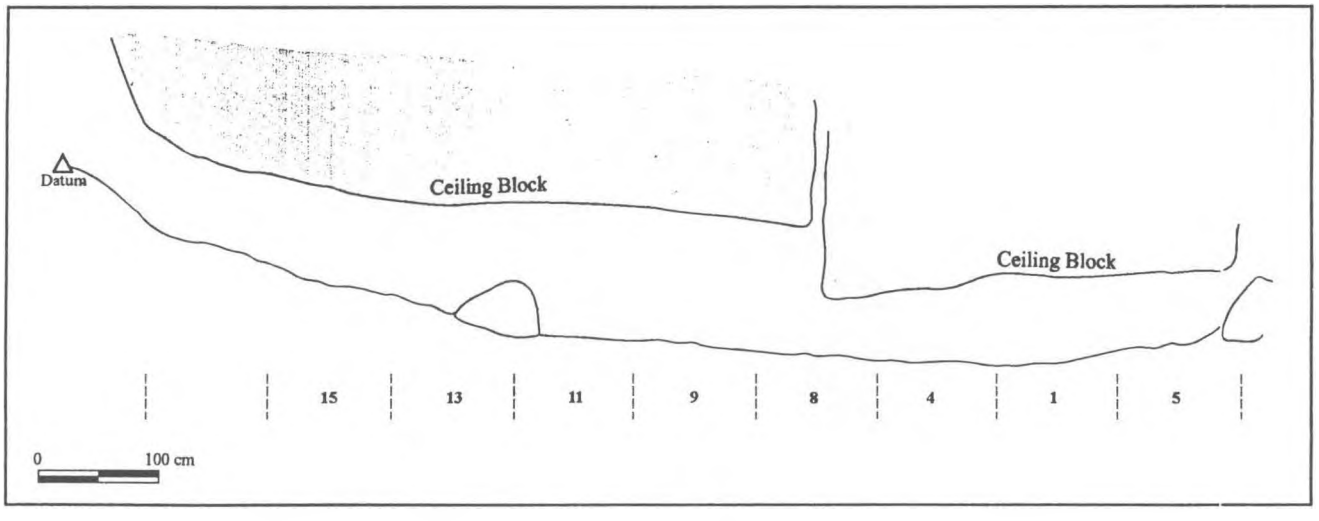

Figure 8.4 DgRw 199-F1: cross-section of burial chambers.

EU 1 from the 1992 project coincides with Skinner's 1987 test unit 7.5-8.5S, which he excavated to a maximum depth of 25 cm below surface, at which point he reports encountering bedrock along the south margin of the unit. In 1992 we were able to excavate another 15 cm in this unit, which was found to contain the deepest deposits in the entire east chamber.

Matrix Description

Stratigraphic profiles were drawn at two locations in 199-F1, 4.5 m east (east wall of EUs 11 and 12), and 6.5 m east (east wall of EUs 7 and 8), to illustrate the sequence of cultural deposits in the west and east chambers, respectively. Four major stratigraphic layers were identified in the profiles (Figure 8.5).

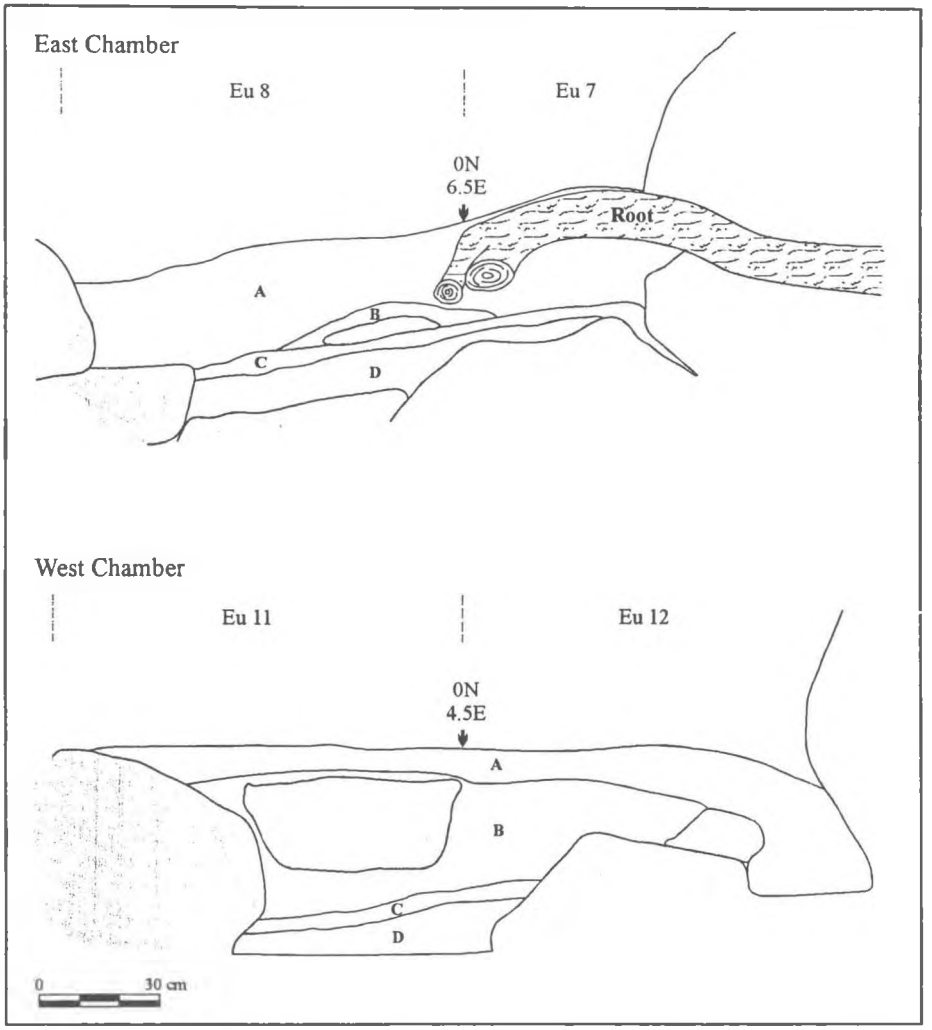

Figure 8.5 DgRw 199-F1: stratigraphic profiles at 6.5 and 4.5 m east.

Layer A: organic dark yellowish brown (10YR 3/6) to dark brown (10YR 3/3) loose, dry, silty sand with abundant sandstone and conglomerate rubble intermixed with decaying leaves, wood, bark, roots and rootlets. Small amounts of marine shell, land snail, and both burnt and unburnt human bone are present, along with occasional charcoal chunks, probably of modern origin. Lenses of concentrated fish bone occur in EUs 3 and 9. Organic litter is most prevalent along the west entrance passage and adjacent EUs, and near the middle of the feature below the crack between the two ceiling blocks. Layer A ranges in thickness from <10 cm in the west chamber, to 30 cm in the east-central region.

Layer B: very dark brown (10YR 2/2) to black (10YR 2/1) moist, moderately compact silty sand mixed with sandstone and conglomerate rubble ranging in size from cobbles to boulders. Constituents include abundant marine shell (mainly clam and/or mussel), fish bones (sometimes in discrete lenses), and highly fragmented burnt human bone. Stains, flecks, and small chunks of charcoal were noted throughout, but no fire-altered rocks (FAR) were observed. Roots are still frequent. This layer predominates in the west chamber, where it reaches depths of >30 cm; in the east chamber it is considerably more shallow, and is limited in extent to the western half of the chamber.

Layer C: a thin layer of dark brown (10YR 3/3) to very dark greyish brown (10YR 3/2) moist, slightly silty sand containing decayed conglomerate rubble and small to huge sandstone slabs. Fish bones, marine shell, and human remains are still common, but less frequent than in Layer B. Charcoal flecks and chunks occur throughout, but no FAR was found. Root penetration continues. Layer C extends throughout both chambers, but is less than 10 cm in thickness.

Layer D: dark yellowish brown (10YR 4/4) to brownish yellow (10YR 6/6) compact, moist silty sand with sandstone slabs and conglomerate cobbles and boulders. This layer contains no shell, fauna, human remains, or charcoal, although roots and rootlets are still common.

Faunal Remains

The faunal assemblage from DgRw 199-F1 is derived from four sources: Skinner's 1987 project; the 1992 excavations; and two matrix samples (MS) collected from the east (EU 3) and west (EU 9) sides of the feature, also in 1992. Skinner's sample consists of 552 shell fragments and 69 skeletal elements either surface-collected from the main cave or excavated from the fissure area and the upper levels of EU 1 (Skinner 1991: 73-74, 94-96). It comprises less than 1% of the total faunal assemblage, and contains no unique or unusual specimens. Because methods of collection and analysis differ from the current study, it is not directly comparable to the rest of the faunal assemblage, and will not be considered in detail. The 1992 excavation sample consists of all non-human skeletal remains recovered during the excavation of EUs 1-16; it comprises 10,555 specimens, or approximately 40% of all vertebrate fauna from the feature. MS-3 yielded 11,440 vertebrate specimens (43.3% of the assemblage), compared with 4,378 (16.6%) from MS-9. Detailed catalogues of the excavated and matrix sample fauna may be found in Appendix A, Tables A.7-A.9. The following discussion summarizes the results of the faunal analysis undertaken by van Gaalen (1994) and Kusmer (1992).

Fish remains dominate all four samples, and comprise more than 90% of the total vertebrate assemblage (Table 8.1). Only 11% of the excavated sample and less than 5% of the matrix samples could be identified to taxon, but an extraordinary variety of fish are represented in the identified remains. Local, non-migratory fishes, readily procurable year round in the shallow waters, bays, and tidal pools off Gabriola Island, predominate. Common in all three samples are members of the gunnel/prickleback and sculpin families; rockfish and surfperches also occur relatively frequently (>10%) in the excavated sample. Interestingly, in contrast to the burial features at DgRw 204, salmon is virtually absent at DgRw 199-F1, and herring is rare except in MS-9, where it comprises about 16% of the fish sample.

Spatially, fish remains are not randomly distributed throughout the cave: more than half of the excavated fish sample came from EU 9 in the west chamber, and a further 30% came from EU 3, in the east chamber. This pattern is due to the presence of five dense concentrations of fish bones which were discovered during excavation and collected separately: two from levels 4 and 5 of EU 3, and three from levels 2 and 6 of EU 9. These concentrations are comprised of combinations of midshipman, various flatfishes,surf perch, gunnel/prickleback, rockfish, and sculpin, as well as many unidentified fish (van Gaalen 1994). An unusual characteristic of these concentrations is that all of the fish represented are approximately the same size (i.e., all the vertebral centra measure about 2 mm). They include not only small species of fish, such as gunnel, but also immature specimens of larger species of fish, such as rockfish and sculpins. Juveniles of some of these larger species range near the shores from spring to summer, and may have been caught in shallow waters and inter-tidal pools along with the smaller, more permanent residents. The fish are represented by vertebrae, various skull and pectoral elements, and the occasional pelvic portion.

The sheer abundance of fish remains in 199-F1, their occurrence in dense concentrations in specific locations within the cave, and the evidence of burning on some of the specimens, all suggest that these fauna were introduced into the burial cave by human agency, probably in the form of food offerings for the dead. The large number of gunnel/prickleback remains is somewhat puzzling, however, since they are not traditionally known as a food fish (van Gaalen 1994), although they have previously been found in archaeological fauna assemblages (Wigen and Stucki 1988). Perhaps these small fish were collected adventitiously along with other targeted prey, such as rockfish, or perhaps the food requirements of the dead differed from those of the living. Once introduced into the feature, many of the fish offerings were scavenged by carnivores who intermittently inhabited the cave: carnivore chew marks were observed on 1518 fish bones or 6.3% of the collection.

Mammals are the second largest class of vertebrate fauna at 199-F1, representing slightly less than 9% of the assemblage. Of the 2,268 specimens recovered, only 8% could be identified to taxon. Identified mammalian remains from the two matrix samples are almost exclusively those of rodents (rats, mice, voles). The excavated sample is also dominated by rodents (55%), followed by carnivores (25%) including racoons and canids, and ungulates (16.8%), particularly deer. Most of the racoon remains (80%) are from immature individuals, as are approximately half of the deer remains. The canid bones, on the other hand, are predominantly from mature individuals. Mammal remains also exhibit a non-random distribution at the site, with frequencies of $\geq$ 20% in EUs 3, 4, and 9, and $\leq$ 5% in all other excavation units.

Table 8.1 Summary of vertebrate fauna (NISP), DgRw 199-F1.

Sample	Fish	%	Bird	%	Mammal	%	Other	%	Total
1987 Exc.	58	84.06	3	4.35	8	11.59	0	0.00	**69**
1992 Exc.	9,856	93.38	149	1.41	540	5.12	10	0.09	**10,555**
MS-3	10,299	90.03	14	0.12	1,125	9.83	2	0.02	**11,440**
MS- 9	3,771	86.14	11	0.25	595	13.59	1	0.02	**4,378**
Total	**23,984**	**90.70**	**177**	**0.67**	**2,268**	**8.58**	**13**	**0.05**	**26,442**

Other = reptile & amphibian.

Both natural and cultural processes contributed to the mammalian assemblage at 199-F1. The majority of these remains, particularly the rodent, rabbit, racoon, and canids, probably represent natural accumulations, but the presence of cut marks, spiral fractures, and evidence of burning on some elements points to human intervention in some cases.

Avian fauna are scarce at 199-F1, contributing less than 1% to the total vertebrate assemblage (n=177 specimens). Approximately 40% of the specimens, the majority of which came from the excavated sample (n=72), could be identified to taxon. Most common are grouse (29.7%) and waterfowl (29.7%), especially ducks. A variety of perching birds are also represented, including crow, raven, finch, blackbird, and thrush. Identified elements include wing and leg bones, vertebrae, and the occasional skull/mandible, sternal, and pelvic portion (van Gaalen 1994). Two chicken bones attest to the presence of modern or recent inclusions in the cave. Evidence of spatial patterning in the distribution of avian fauna is less clear than for the fish or mammal remains, but the densest concentration also occurs in EU 3 (20.8%). The other excavation units each contribute less than 8% to the bird assemblage, except for EU 4 (14.1%), EU 13 (12.1%), and EU 9 (11.4%).

Most of the identified bird species are not cavern dwellers or nesters, and therefore must have been brought in by an outside source. The gull, falcon, pigeon, and perching birds probably represent carnivore prey, whereas the waterfowl and grouse are more likely to have been introduced by humans. Some of the bird remains exhibit evidence of human intervention, in the form of burning and spiral fractures.

The remainder of the faunal assemblage consists of a few snake and frog/toad remains.

Stratigraphically, the vertebrate fauna exhibit a bimodal distribution, with peak frequencies near the surface (levels 1 and 2) and near the middle (levels 5 and 6) of the deposits (Table A.11). To a large extent this reflects the vertical distribution of fish remains, the most common class of vertebrate fauna, and in particular the fish concentrations in EUs 3 and 9. Mammalian and avian fauna from the excavated sample occur in peak frequencies in level 2 and decline steadily in frequency with increased depth below surface. Too few bird remains were recovered from the matrix samples to detect patterning in their vertical distribution, but the mammal distributions differ slightly: in MS-9 they decline steadily from a peak in level 1, whereas in MS 3 they are most frequent in level 3.

Invertebrate fauna in the form of fragmented shell is very common at 199-F1. Identified taxa include bay mussel (*Mytilus edulis*), Pacific little neck clam (*Protothaca staminea*), horse clam (*Tresus* sp.), butter clam (*Saxidomus giganteus*), basket cockle (*Clinocardium nuttalii*), barnacle (Subclass Cirripedia), limpet (Acmaeidae family), periwinkle (Littorinidae family); crab (Order Decapoda), whelk (*Thais* sp.), sea urchin (Class Echinoidea), and Oregon forest snail (*Allogona townsendiana*) (Kusmer 1992). To estimate the relative frequency of invertebrate fauna, all shell remains were extracted from the two matrix samples, identified to taxon, and weighed (Tables A.12 and A.13). The two matrix samples show different distributional patterns. In MS-3 shell is relatively scarce at the bottom of the deposits, abruptly increases in frequency to a maximum in level 5, then declines steadily to a minimum in level 1. In MS-9 invertebrate remains are most abundant at the bottom of the deposits, and decline steadily in frequency to reach a minimum, like MS-3, in level 1. The two samples also differ in composition: MS-3 is dominated by mussel, except in level 2 where varieties of clam are more common; in MS-9 mussel dominates only in the lower three levels of the deposits, after which it is gradually replaced by clam species, until, in the upper two levels of deposits varieties of clam are virtually the only invertebrate fauna recovered.

Artifacts

DgRw 199-F1 has yielded a total of 148 artifacts and artifact fragments, eight of which were recovered in 1987 (Skinner 1991: 52-54, 71-72), and 140 in 1992. The majority (79%) came from the west chamber, but small numbers of artifacts were also recovered from the east chamber (13%), EU 16 (4%), and the "fissure" (4%). Although artifacts were recovered from every level of the deposits, the greatest number (63%) came from levels 3-5 (10-25 cm BS), which also coincides with the densest concentration of human bone. A variety of materials was used in the manufacture of these items, including antler, stone, bone, shell, copper, and wood. Some of the artifacts are complete, but many have been burnt and broken, perhaps deliberately, so that the number of worked fragments (148) is considerably larger than the number of identified artifacts (89). It was often possible to reconstruct pieces of the same object, or to ascertain that fragments were from the same artifact, even when the pieces did not articulate. The artifacts are discussed briefly below; complete descriptions and illustrations may be found in Appendix B.

Antler. Distinguishing antler from bone was sometimes difficult given the highly fragmented and burnt condition of the majority of the specimens. However, 52 items were identified as antler, including one badly weathered, long, slender, unilaterally barbed point decorated with incised parallel lines down the long axis of the shaft (Figure B.7a). This was the only complete antler artifact. The remaining 51 antler specimens represent fragments of at least three different artifacts: another decorated barbed point (41 small fragments, Figure B.7b-q), an elaborately carved piece of art with a curvilinear design (6 pieces, Figure B.5), and a spoon (?) with a zoomorphic design carved in relief on the handle (2 pieces, Figure B.6). Two miscellaneous worked fragments complete the antler collection.

Bone. The 25 pieces of worked bone recovered from 199-F1 can be divided into two categories: tools, and modified objects of no known utilitarian function. Among the tools are three small, carefully worked unipoints (Figure B.4g-i), a harpoon foreshaft (Figure B.4a), and a whale bone bark shredder (Skinner 1991: Figure 13), all of which are unburnt. Burnt bone tools include an awl tip (Figure B.4e), a ground, faceted point fragment (Figure B.4f), and 12 ground and polished fragments of an unusual object with longitudinal grooves carved on opposite surfaces (Figure B.4l-o). Seven of the pieces articulate with others, but not enough of the artifact is reconstructed to determine its ultimate shape or function. The remaining modified bones include a ground canid maxilla (Skinner 1991: Figure 8), two small cut and smoothed skull sections, and three very small long bone pieces with smoothed edges and polished surfaces.

Shell. The artifact assemblage includes twenty-two items made of shell, most of which are ornaments. The majority (n=13) are dentalium beads or bead fragments, including one carved with a zigzag geometric pattern (Figure B.8i-m). The remaining shell ornaments are three small rectangular pendants (Figure B.8e, f, h), made of clam, abalone, and California mussel shell, and an unusual, finely-worked U-shaped object, possibly a nose ornament (Figure B.8n).

In addition to the ornaments, three fragments of scallop shell (*Pecten caurinus*), possibly pieces of a ritual rattle, were recovered (Figure B.8c-d). The final two modified shell objects are fragments of California mussel and unidentified clam shell with ground or sectioned edges but no discernible shape or function.

Stone. The forty-five stone artifacts include 19 decorative items, 11 tools, 5 obsidian microblades (Figure B.3s-v), 7 pieces of lithic detritus, 1 utilized flake, and 2 ground stone fragments. The decorative pieces are all personal ornaments: 12 beads (disc and barrel-shaped, Figure B.3g-r), 6 ground stone ovals perforated at both ends (Figure B.3a-f), and a thin siltstone disc with two perforations (Figure B.3y), which Skinner (1991) referred to as a button, but which may be a pendant. With the exception of the "button" and one mudstone bead, all of the ornaments are made of soft black stone (steatite?) or cannel coal. Several of the decorative items are very friable, and appear to be burnt; one is reconstructed from two fragments recovered from different excavation units. These artifacts have restricted distributions within the feature: all of the barrel beads came from the west-central area (EUs 8, 9, and 10); all of the disk beads from the east-central area (EUs 3, 4, and 7); and all of the perforated ovals from the west end (EUs 11, 12, and 14).

The stone tools include a thin ground slate knife fragment (Figure B.1i), two nephrite or greenstone adze blades (Figure B.2a, c), a small tear-shaped chipped chert point (Figure B.1a), a stemmed chipped basalt point (Figure B.1c), a ground slate point fragment (Figure B.1e), a sandstone atlatl weight (Figure B.2g), two small triangular sandstone abraders (Figure B.2c, d), a large wedge-shaped abrasive stone, and a hammerstone. The lithic detritus includes five platform-bearing flakes, one flake shatter, and wedge-shaped piece of block shatter; most are made of medium to coarse-grained basalt, but quartzite, quartz

Table 8.2 Radiocarbon dates from DgRw 199-F1.

Lab Number	Item	Provenience	Measured C-14 Age [2]	Conventional C-14 Age [3]
TO 11451[1]	zygoma	EU 1 Surface	2760 ± 60	
SFU 546	ribs	EU 1 Level 1-5	2420 ± 70	
SFU 610	misc. bone	Fissure	2170 ± 70	
SFU 542	burnt wood	EU 1 Level 1-5	760 ± 65	
BETA-74076[1]	fibula	EU16 Level 4	3120 ± 50	3240 ± 50
BETA-90639[1]	mandible	EU13 Level 3	1260 ± 40	1400 ± 40

[1] AMS date.
[2] radiocarbon years before present (AD 1950); 1 sigma, 68% probability.
[3] conventional C-14 age, corrected with reference to measured C13/C12 ratio; 1 sigma, 68% probability .

porphyry, and greywacke were also employed. The remaining two items are a small nephrite block with one ground and polished surface, and a coarse reddish sandstone block with one highly polished surface.

Copper. The single copper artifact is a small, thin, rectangular ornament with a drilled perforation at one end (Figure B.3z).

Wood. One possible wooden artifact was collected: a slender cedar stake with one end bifacially ground to a blunt point. This object is very similar to a cache of worked cedar stakes discovered near DgRw 213 during the 1989 burial reconnaissance.

Dating

Skinner obtained four radiocarbon dates on materials from 199-F1, including three bone samples (a pathological skull from the surface of the main cave, a rib sample from EU 1, and a miscellaneous bone sample from the fissure area), and one piece of charred wood, also from EU 1 (Skinner 1991: 47). During the current study, two additional bone dates were obtained, on a fibula fragment from EU 16 and a child's mandible from EU 13. Dates obtained are presented in Table 8.2.

Based on these dates it appears that 199-F1 experienced a long history as a burial site, perhaps a thousand years or more. The "west crevice" area (EU 16), just inside the entrance to the main cave, was utiized first, in late St. Mungo or early Locarno times, followed by the main cave (Locarno age), and finally the fissure area (Marpole age). The two outlying dates require some explanation. The date of 1400 ± 40 obtained on the child's mandible from EU 13 almost certainly underestimates the true age of the burial, as a result of contamination by fine rootlets that could not be effectively removed before dating (Darden Hood, personal communication 1996). The origins of the burnt wood sample that yielded the youngest date are unclear: it may be from a burnt root, or wood introduced during a later intrusion into the cave, perhaps by a curious passer-by, or by descendants of the deceased bringing food to their ancestors

Human Remains

Feature 1 yielded the largest human skeletal assemblage of all the burial features investigated on the False Narrows bluffs, a total of 159,323 bones, teeth, and fragments, including 1,178 specimens collected by Skinner in 1987. The number I have cited here differs slightly from the total of 1,098 reported by Skinner (1991), due mainly to the presence of multiple fragments assigned a single catalogue number. None of the elements recovered *in situ* were articulated in anatomical position, but several bone clusters sorted by element (skulls, mandibles, humeri, ulnae, innominates) were found in deep deposits near the entrance passage (EUs 13 and 15).

The assemblage from 199-F1 is characterized by extreme fragmentation: 51.7% percent of the recovered specimens (n=82,330) were too small to be identified to skeletal element, and were merely counted and bagged according to provenience. The extreme fragmentation may be due in part to the frequency of foot traffic through the feature, including a minimum of three archaeology field crews and at least one organized archaeological tour (William Paull, personal communication 1989), as well as numerous tourists, local residents, and casual visitors to the area. Despite the degree of fragmentation, most skeletal elements are well represented in the human bone assemblage, particularly the cranial remains that are so uncommon at DgRw 204 (Table C.1).

Condition

With the possible exception of DgRw 204-F6, the human remains from 199-F1 are the most poorly preserved of all those collected in the course of the project. Only 3.5% of the recovered elements were assessed as being in good condition, while more than

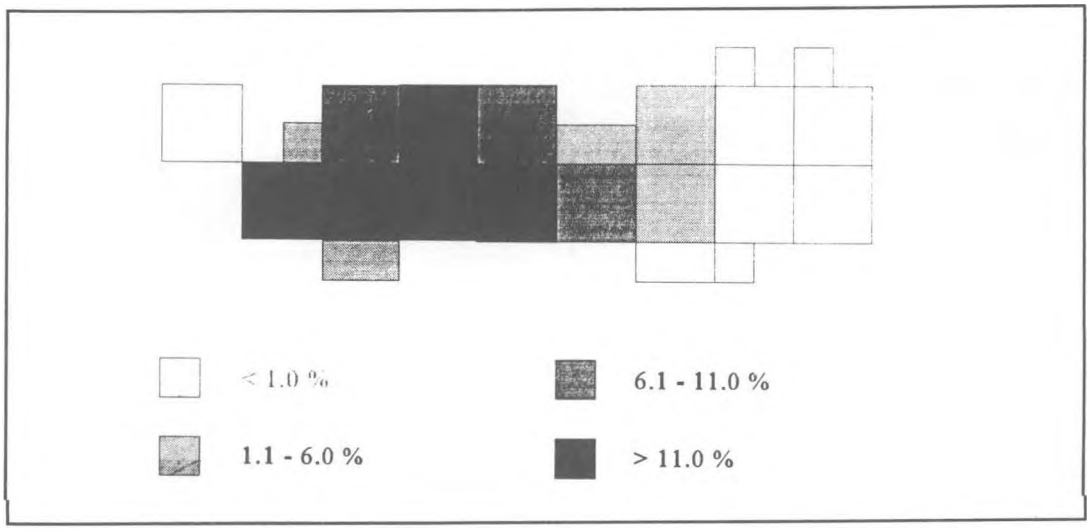

Figure 8.6 Horizontal distribution of human remains, DgRw 199-F1.

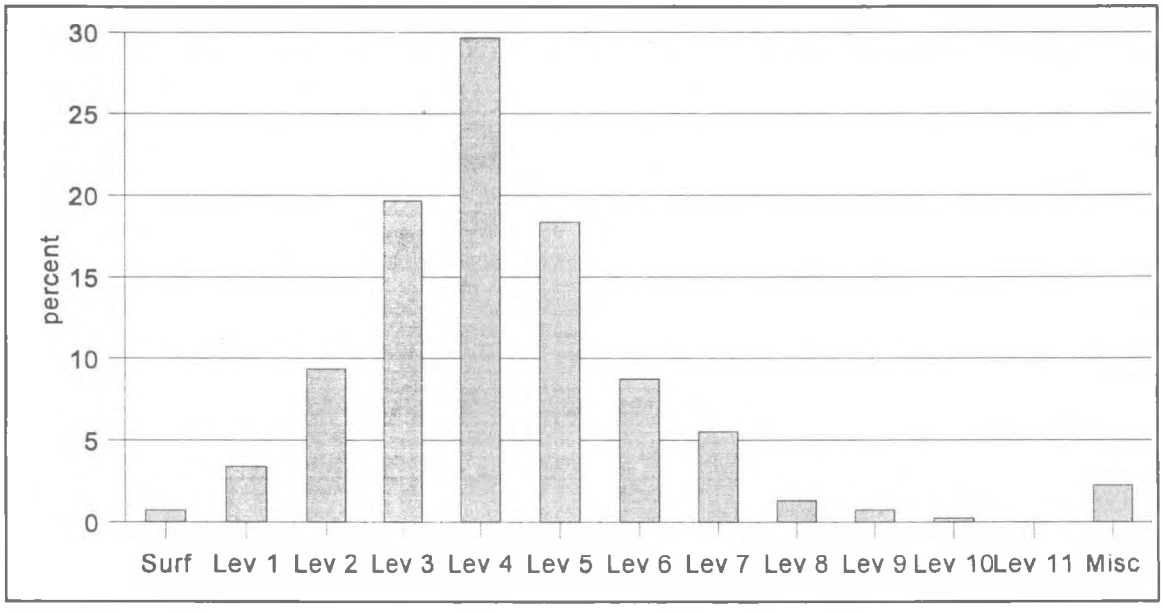

Figure 8.7 Vertical distribution of human remains, DgRw 199-F1.

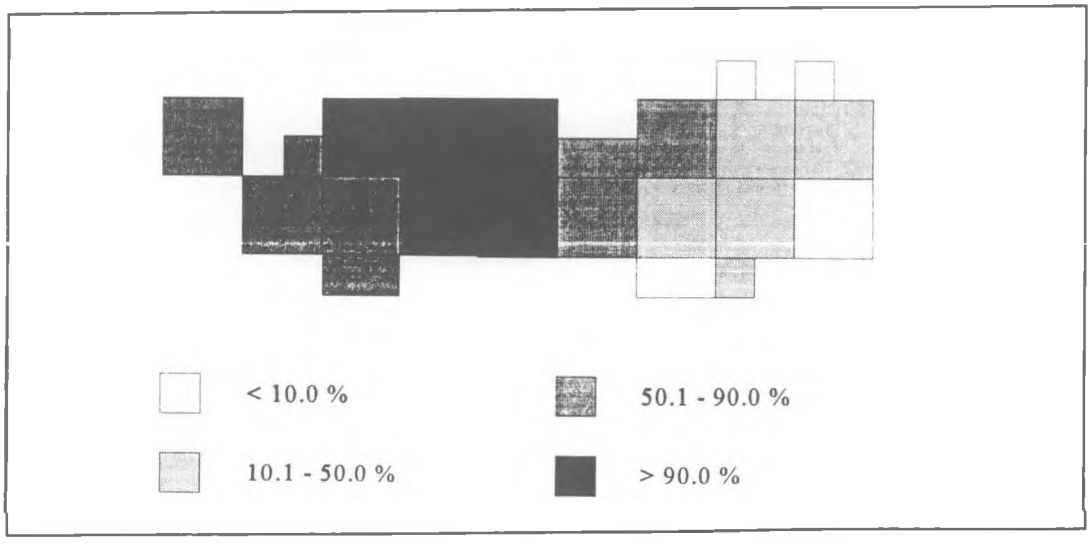

Figure 8.8 Horizontal distribution of burnt human bone (% of unit total).

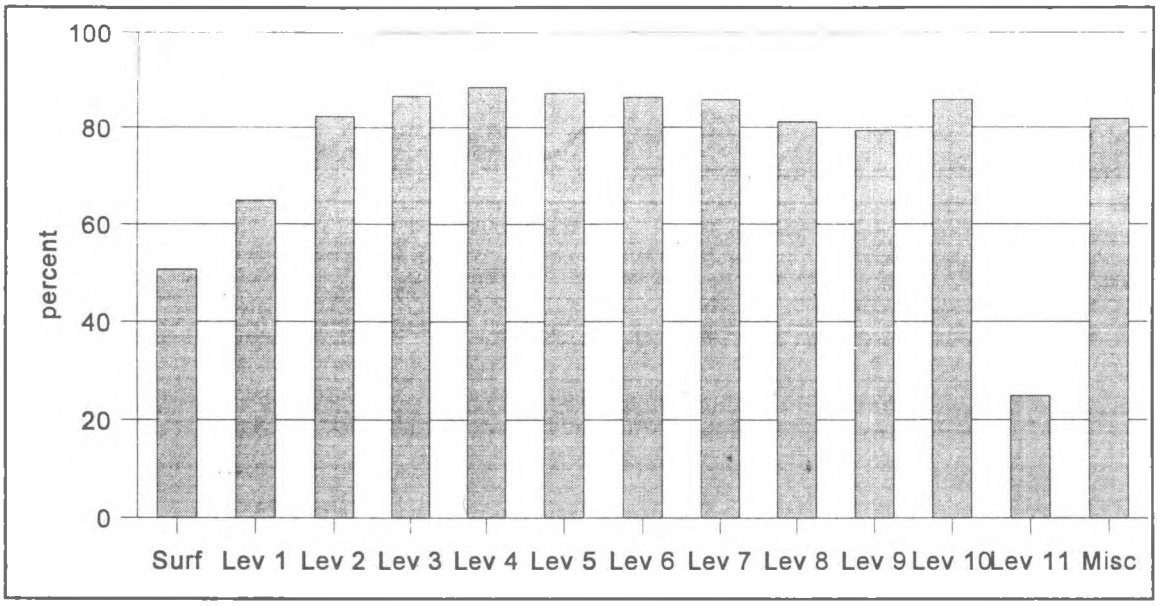

Figure 8.9 Vertical distribution of burnt human bone (% of level total).

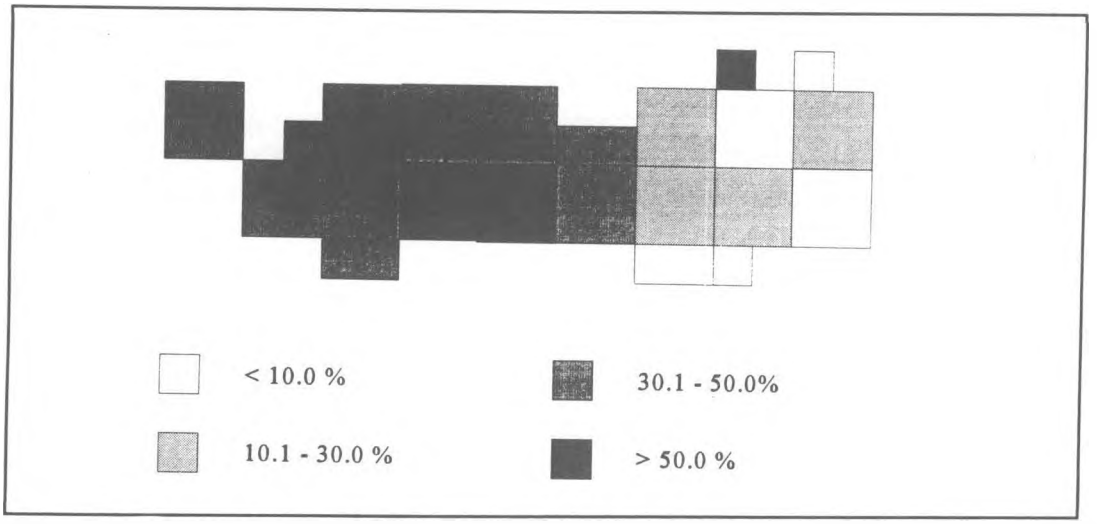

Figure 8.10 Horizontal distribution of calcined human bone (% of burnt total).

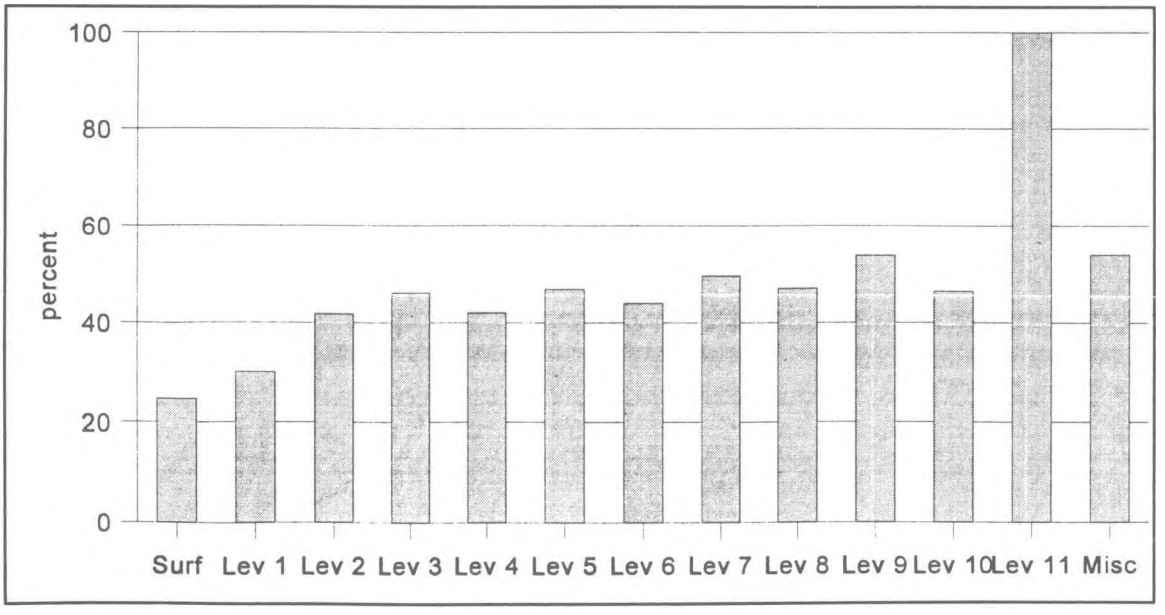

Figure 8.11 Vertical distribution of calcined human bone (% of burnt total).

two-thirds were deemed poorly preserved. Few skulls or long bones were found intact, and the frequency of unidentifiable pieces (51.7%) attests to the high degree of fragmentation. Areas of the skeleton with thinner cortical bone were particularly prone to post depositional damage, with the result that cranial remains typically consist of calvaria lacking facial elements, and long bones are usually represented by diaphyses, with metaphyses and articular surfaces damaged or missing. This pattern of survival is directly correlated to regional differences in bone mineral density throughout the skeleton (Willey et al. 1997), and is not thought to reflect mortuary treatment or deliberate *post mortem* modification, such as cannibalism (e.g., White 1992). Teeth are frequently broken (or completely shattered if burnt), and even the more complete specimens often have large areas of enamel exfoliated.

Bone preservation was best (23% - 67% in "good" condition) at the extreme east end of the feature (EUs 1, 2, and 6; EXs 2N and 6N) and worst (<5% in "good" condition) in the west chamber near the main entrance. This difference may be due to the higher amounts of traffic through the more accessible and spacious west chamber. State of preservation is not consistently correlated with depth of burial, although the cause of the damage may be: surface remains are more likely to be "weathered" (expressed as cortical pitting and erosion), while subsurface remains are more subject to root damage, in the form of surface etching and/or medullary penetration with subsequent destruction of adjacent cancellous bone.

Of the skeletal remains recovered in 1992, 986 specimens (0.62%) exhibit some degree of calcareous plaque, usually in small discontinuous patches on exposed surfaces. Occurrence of the plaque appears to be correlated with proximity to chamber walls and ceiling, with the highest frequency (>5% of fragments affected) along the south wall of the east chamber (EUs 1, 4, and 5) where the ceiling is lowest, and in EU 16, a small, natural stone cist. Two other relatively enclosed areas, the entrance tunnel (EU 15) and the constricted neck between the east and west chambers (EUs 7 and 8) do not exhibit the expected frequencies of calcareous plaque, probably because both are open to the outside (the former through the main entrance, the latter through a large crack between the two ceiling blocks), and subject to increased sedimentation and the accumulation of forest litter which presumably would bury fragments before the mineral precipitate could develop. Affected fragments are most common on the surface and in the upper levels of the deposits (88.6% in levels 1-4), and decrease in frequency with increased depth below surface.

Thirty-two bone fragments are marked by areas of bluish-green staining, probably the result of contact with copper artifacts. With one exception (from EU 16), all of these pieces came from the west chamber, and most (n=25, 78%) were found in adjacent EUs 11 and 12, in excavation levels 3 and 4 (10-20 cm BS). The only copper artifact recovered from the feature also came from EU 12, level 3. It is unlikely that this small artifact could be responsible for all the copper-staining observed, particularly in bones located one or two metres distant, which raises two possibilities: (1) that additional copper artifacts were once present, but have been removed by looters; or (2) that the copper-stained bone fragments originally were more clustered in space, but have been scattered as a result of some post-depositional disturbance. These possibilities will be explored in greater detail below. The affected pieces are all heavily burnt (calcined) long bone and skull fragments, and may be from a single adult individual.

Four additional bone fragments exhibit reddish-orange staining suggestive of ochre, but no pieces of ochre were recovered during the excavations. The stained bones come from the west chamber, EUs 9, 11, and 12, excavation levels 3-5.

Evidence of modification by animals was observed on 127 specimens, 23 of which (18%) were gnawed by rodents and 104 (82%) chewed by carnivores. The rodents exhibit a preference for articular surface margins and bony ridges and projections, such as orbital margins, zygomatic arch, ascending ramus of the mandible, and *linea aspera* of the femur. Carnivore damage, on the other hand, was more common in parts of the skeleton with thin cortical cover over underlying cancellous bone, including ribs, vertebrae, innominates, and the metaphyses of long bones. Both rodents and carnivores show a predilection for unburnt bones: 84% of affected specimens are unburnt, and another 9% are only slightly burnt.

Human-induced bone modifications in the form of cutmarks were observed on 94 specimens (0.06% of the assemblage). The toolmarks tend to occur as clusters of short, parallel, narrow incisions with V-shaped cross-sections, apparently produced by a slicing or back-and-forth sawing motion, rather than hacking or battering. The skeletal element most commonly affected is the skull (n=43, 45.7%), followed by rib (n=4, 4.2%), vertebra (n=4, 4.2%), femur (n=3, 3.2%), innominate (n=3, 3.2%), humerus (n=2, 2.1%), scapula (n=2, 2.1%), and single instances of clavicle, ulna, tibia, 3rd cuneiform, triquetral, third metacarpal, and middle hand phalanx. The remaining 26 specimens are unidentified long bone shaft fragments, most of which come from large-diameter long bones such

as the femur, humerus, and tibia. The majority of the cut specimens are from adults (n=82, 87.2%), but child (n=7) and infant (n=3) remains are also affected, as well as two additional fragments from unaged subadults.

Interpretation of cutting patterns is hampered by the small size and undifferentiated morphology of the majority of the specimens. Most of the affected cranial (n=32) and long bone (n=26) fragments could not be attributed to a specific skeletal element, much less to a particular region of an element. In those instances where such attributions are possible, however, cutmark location seems indicative of skeletal dismemberment, specifically decapitation (mastoid process, atlas vertebrae), and disarticulation of the mandible (severing of *masseter* and *temporalis* muscles), shoulder (circum-glenoid region of the scapula), and elbow (distal humerus). Additional transverse cutmarks across the mid-frontal squama, frontal bosses, mid-coronal sutures, and inion region of the occipital may be indicative of *peri mortem* scalping, which has been documented elsewhere in Coast Salish territory in the prehistoric period (Curtin 1992). The origins of the remaining cutmarks are unclear, but *peri mortem* violence is a possibility: cutmarks on finger and metacarpal shafts may be defensive wounds, while cutmarks along the iliac crest and anterior superior iliac spine would sever the oblique muscles of the abdomen, and may be evidence of disembowelment.

A second form of human-induced modification, burning, is discussed at greater length below.

Spatial Distribution

The spatial distribution of the human remains is summarized in Table 8.3 by excavation unit and level. The column labelled "?" refers to specimens for which the vertical provenience is uncertain, including Skinner's excavated material from levels 1-5 of EU 1 (his unit 7.5-8.5S), and material collected from the slumped levels 5-8 in EUs 8, 10, 11, and 12.

The majority (77.2%) of the surface remains encountered in 1987 were found in the east chamber of the burial cave, but as Figure 8.6 illustrates, when the assemblage is considered as a whole, human remains are most densely concentrated in the west chamber. This is due in part to the greater depth of deposits in the west chamber, which have more potential for subsurface remains, but it is also possible that surface remains were deliberately moved from the west to the east chamber by some of the recent visitors to the cave, to clear a space for whatever activities were held there. When Skinner visited in 1987 he found numerous skulls and other bones heaped in a pile in the vicinity of EU 1.

Human remains were found to a maximum depth of 55 cm below surface, but the majority (67.7%) were found from 10-25 cm below surface in levels 3-5 (Figure 8.7)

Burning

The majority of the human bones collected from 199-F1 exhibit some evidence of burning. Although this attribute was not scored for most of the small, unidentified fragments, of the 88,832 specimens for which the information was collected (55.8% of the total assemblage), a total of 75,662 (85.1%) were burnt to some degree. There is definite patterning to the spatial distribution of burnt remains, with the east chamber containing predominantly unburnt remains and the west chamber mainly burnt specimens (Figure 8.8). Unburnt skeletal remains tend to be found on the surface or in the first 5 cm of the deposits; below this, burnt remains predominate (Figure 8.9). A sub-sample of 68,353 burnt specimens was scored for intensity of burning, which ranged from slight or localized discolouration, to deep charring, to severe calcination. Nearly half of these (44.3%) were classed as severely burnt or calcined. The vertical and horizontal distribution of severe burning parallels that of burning in general: it is most common in the west chamber of the cave, and below the first level of deposits (Figures 8.10 and 8.11). Both the likelihood and the intensity of burning are strongly correlated with age-at-death: 82.3% of infant remains are unburnt, compared to 50.6% of children, and only 13.4% of adults; severe burning (calcination) was seen in only 10.3% of infant bones, compared with 25.8% of children and 38.7% of adults. Patterns of burning for the five excavated features are compared in Appendix C, Table C.5.

The burnt bones exhibit a suite of traits characteristic of the cremation of fleshed remains or green bones: deep, curved, transverse cracks and fractures often ending in longitudinal hinge terminations, and frequent exfoliation of cortical surfaces, with warping and shrinkage evident in the most severely affected specimens (Binford 1963; Baby 1954; Buikstra and Swegle 1989). Only one long bone shaft fragment (humerus/ femur) displayed the distinctive colour pattern identified by Buikstra and Swegle (1989) as indicative of the intense burning of dry bone: light brown to tan coloured outer cortex overlying black, grey, or white inner cortex and trabeculae. This interpretation is further supported by evidence of differential burning within elements that can be attributed to the shielding effects of muscle cover. Three ulnae, for example, are unburnt except for their distal shafts which are discoloured to charred. Two femurs have

Table 8.3 Spatial distribution of human remains, DgRw 199-F1.

Unit	Surf	Lev 1	Lev 2	Lev 3	Lev 4	Lev 5	Lev 6	Lev 7	Lev 8	Lev 9	Lev 10	Lev 11	?	Total	%
1	147					52	123	26	6				309[1]	663	0.42
1SX		26	7											33	0.02
2	13	62	75	15	13	2	4							184	0.12
2NX			13											13	0.01
3	19	370	424	474	589	78	28	2						1,984	1.25
4	192	517	523	819	1,044	133	11	7						3,246	2.04
4SX		85	57											142	0.09
5	3	15	10	5										33	0.02
6		15	13	6	1									35	0.02
6NX					1	2								3	0.00
7	15	61	178	401	846	3,103	822	1,095	134	43				6,698	4.20
8	122	192	520	1,003	4,768	2,972	378	690	35	2			346[2]	11,028	6.92
9	28	2,346	2,475	6,811	7,650	1,651	411	91	22				4	21,489	13.49
10	423	329	1,356	2,620	2,144	3,159	484	199	14				101[2]	10,829	6.80
11	13	760	3,887	7,370	7,255	690	341	54	94	27			234[2]	20,725	13.01
12	56	438	1,837	7,534	5,046	2,057	368	1,320	84	43			2,049[2]	20,832	13.08
13	4	11	52	743	9,052	5,441	2,989	3,107	950	472	177	3		23,001	14.44
13SX		4	55	123	176	183	583	1,196	343	111	45	1		2,820	1.77
14	5	182	3,371	3,076	2,443	1,347	818	39	7	13			34	11,335	7.11
15	1	10	16	78	5,993	7,152	4,612	427	79	465	153			18,986	11.92
15NX	4					1,047	1,910	387	186					3,534	2.22
16	2	33	45	221	237	160	48	174	145					1,065	0.67
Misc [3]													194	194	0.12
Fissure													337	337	0.21
Gallery	114													114	0.07
Total	**1,161**	**5,456**	**14,914**	**31,299**	**47,258**	**29,229**	**13,930**	**8,814**	**2,099**	**1,176**	**375**	**4**	**3,608**	**159,323**	100
%	0.73	3.42	9.36	19.65	29.66	18.35	8.74	5.53	1.32	0.74	0.24	0.00	2.26	100	

[1] Material excavated by Skinner from top 25 cm of deposits; no vertical proveniences available.
[2] Material recovered from slumped deposits, levels 5-8; no exact vertical provenience available.
[3] Material recovered from re-screened backdirt; no vertical or horizontal provenience available.

unburnt proximal shafts and burnt distal metaphyses. Tibias tend to exhibit more intense burning on the anterior crest. Frontal and facial bones are generally more heavily burnt than the inferior occipital. In all cases, the effects of burning are more pronounced on the more superficial regions of the skeleton.

It is difficult to extrapolate from the frequency of burnt bone fragments to the frequency of cremated bodies. Although approximately 85% of the catalogued specimens were burnt it does not follow that 85% of the bodies interred in the burial feature were cremated, because burnt bones are more likely to be broken into small fragments, thus inflating the frequency of burnt specimens relative to unburnt ones. A survey of 30 skeletal elements (long bones, carpals, and tarsals) reveals that anywhere from 27% to 83% of the identified elements were scored as unburnt (mean = 54.6%). It does not necessarily follow, however, that because one long bone was unburnt that the body from which it came was not exposed to fire to some extent. Several of the crania and long bones appear to be completely unburnt except for one or more very small, localized patches of charring. In these cases it may be that the burning employed as part of the mortuary ritual was more symbolic than complete.

Table 8.4 Summary of reconstructed skeletal elements, DgRw 199-F1.

Element	Sets	% Sets	Pieces	% Pieces
Skull	643	18.72	3484	29.15
Mandible	125	3.64	490	4.10
Vertebra	286	8.33	690	5.77
Rib	235	6.84	638	5.34
Sternum	12	0.35	36	0.30
Clavicle	30	0.87	81	0.68
Scapula	51	1.48	139	1.16
Humerus	117	3.41	629	5.26
Radius	43	1.25	149	1.25
Ulna	56	1.63	227	1.90
Carpal	10	0.29	21	0.18
Metacarpal	49	1.43	105	0.88
Hand phalanx	74	2.15	158	1.32
Sacrum	14	0.41	37	0.31
Innominate	81	2.36	229	1.92
Femur	150	4.37	950	7.95
Patella	10	0.29	22	0.18
Tibia	76	2.21	418	3.50
Fibula	77	2.24	335	2.80
Tarsal	42	1.22	92	0.77
Metatarsal	70	2.04	159	1.33
Foot phalanx	13	0.38	26	0.22
Radius/ ulna/fibula	320	9.32	828	6.93
Humerus/ femur/tibia	814	23.70	1,907	15.96
Long bone	24	0.70	66	0.55
Misc. articular surface	13	0.38	36	0.30
Total	**3,435**	**100.00**	**11,952**	**100.00**

Skeletal Reconstruction

The more than 150,000 bone fragments recovered from 199-F1 presented a significant challenge in reconstruction. The success rate was determined primarily by time constraints, and it is certain that much more could have been accomplished given unlimited time and personnel. Despite these limitations, a total of 11,952 pieces of bone or tooth (7.5% of the total assemblage, or 15.5% of the identified sub-sample) were found to conjoin with other fragments, yielding 3,435 reconstructed "sets" consisting of from 2 to 99 fragments. Greatest success in terms of both numbers of reconstructed sets and numbers of conjoined pieces was achieved for the skull and for undifferentiated large-diameter long bones (humerus, femur, tibia) (Table 8.4). The majority of the reconstructed sets are very small: about two-thirds contain only two articulating fragments, and 90% are comprised of five or fewer pieces. A small number (n=13) of the sets are very large, however, with more than 50 conjoined pieces. All of the very large sets consist of reconstructed crania.

In general there appears to have been very little scattering of broken pieces of the same bone. In more than 80% of the conjoined sets, all members came from the same or adjacent provenience units (TS scores 2-3), and less than 1% showed substantial dispersal (TS > 10). Vertical and horizontal dispersal scores are very similar, although fragments are slightly more likely to be dispersed vertically (mean = 1.5) than horizontally (mean = 1.3); 93.6% of conjoined pieces come from the same or adjacent quadrants, whereas 87.2% are from the same or adjacent levels. Maximum vertical dispersal (10) is less than maximum horizontal dispersal (15) because the former measure is limited by the depth of the cultural deposits, which is less than their horizontal extent. The distribution of dispersal scores is presented in Figure 8.12, and compared with the other excavated features in Table C.2.

Thirty conjoined sets with very high total scatter scores (TS > 10) were examined in greater detail for the information they could provide about post depositional taphonomic processes in the burial feature. These 30 sets can be grouped into three categories, defined by their dispersal values and the inferred agent of dispersal. Type I sets have high horizontal and low vertical dispersal values, and appear to have been scattered shortly after being deposited in the cave. Their members are found at moderate depths below surface (levels 3-6), in the densest bone deposits, and are scattered horizontally from one end of the cave to the other. Elements from one set (an immature skull) exhibit carnivore chew marks, a good indication of the source of the disturbance. Alternatively, the fragments may have been dispersed through deliberate scattering when initially deposited in the feature.

Type II sets, in contrast, show greater vertical than horizontal dispersal, with some pieces recovered from moderate depths (the dense bone layer) and others from very deep levels, often in EUs 13, 14, and 15. This pattern is probably the result of the natural downward filtering of some elements through cracks on the boulder-strewn cave floor.

Type III sets are dispersed both vertically and horizontally; typically some of their members were

found at moderate to deep levels of the deposits (mainly EUs 4, 7, 9, 10, 13, and 14) while others were found scattered on or near the current ground surface some distance away. This pattern is suggestive of recent disturbance from the digging of pits, probably by the pot-hunters who frequented the cave. It is interesting to note that the results of the faunal analysis also indicated recent disturbance to at least 30 cm below surface in EU 9 (van Gaalen 1994).

Demography

Minimum number of individuals (MNI) was calculated for several different skeletal elements, including five of the six major limb bones (the fibula was not considered due to poor preservation and difficulties in siding shaft fragments), scapula, clavicle, atlas, axis, mandible, and petrous portion of the temporal bone. Adults are best represented by the midmandibular region, followed by the odontoid process of the axis vertebra, while subadults are best represented by the frontal bone, mandible, and axis vertebra. The largest estimated MNI derived from a single element is 114, based on a count of 95 adult mandibular symphyses with intact genial tubercles, plus 19 immature mandibles or unfused right hemi-mandibles. This is almost certainly an underestimate of the true number of interments, since at least 21 immature frontal bones are present. When all of the immature dentitions (maxillae, mandibles, and loose teeth) are considered together and seriated by dental development, a total of 23 subadults can be distinguished, which, added to the 95 adults identified by mandibular symphyses, yields a best estimate of 118 individuals represented in this burial feature. It is interesting to note that based on a calculated MNI of 17 individuals among the materials collected in 1987 from the cave surface and the partial excavation of EU 1, Skinner (1991: 57) predicted that the feature might contain as many as 126 individuals, a remarkably accurate estimate given the limited data available to him.

Table 8.5 Adult age estimates, DgRw 199-F1.

Element	Young Adult	%	Middle Adult	%	Old Adult	%	Total
Skull	15	33.3	19	42.2	11	24.4	45
Mandible	14	32.6	17	39.5	12	27.9	43

The subadult remains consist of 14 infants less than two years of age, 7 children between the ages of 3 and 10 years, and 2 older juveniles/adolescents (12-15 years old). Among the infants are five very young individuals, probably newborns, including two possible fetuses between 8 and 9 lunar months in age. Subadult age determinations were based on dental development standards (Trodden 1982; Buikstra and Ubelaker 1994) augmented by skeletal measurements for the possibly fetal remains (Fazekas and Kósa 1978). Although immature remains were recovered from all excavation units in the feature, they are clearly concentrated in the east chamber (Figure 8.13).

Adult age estimates were derived from ectocranial suture closure and dental attrition, since the two best indicators of adult age, the pubic symphysis and auricular surface, were so poorly represented in the assemblage. Degree of suture closure was assessed for 45 adult cranial specimens using the standards of Meindl and Lovejoy (1985). Given the fragmentary nature of some of the cranial remains, only very broad age estimates could be made: young adult (21-35 years), middle adult (36-50 years), and old adult (50+ years). More precise estimates were possible for crania with associated maxillary dentitions, and these skulls were used to determine age category limits among the cranial remains seriated by suture closure. A second set of age determinations based on dental attrition was made for the 43 mandibles and mandible fragments containing teeth. Dental ages were derived from standards established on the prehistoric skeletal sample from the Tsawwassen site (Curtin 1991a). The skulls and mandibles yielded roughly equivalent results (Table 8.5), and show that, unlike 199-F9 (see Chapter 9), a cross-section of adult ages is represented in this assemblage.

Among adults, males and females appear to be present in roughly equal proportions. The best skeletal indicator of sex, the innominate bone, is poorly preserved in this collection; only 29 specimens from each side are suitable for sex determination, providing estimates for less than 1/3 of the adult assemblage. Right innominates include 14 (48.3%) designated male and 15 (51.7%) designated female, while left innominates reveal a definite female bias: 21 (72.4%) female versus only 8 (27.6%) male. Cranial elements are more complete and more abundant at the site, but provide less reliable evidence of sex. Of the 50 complete or partially reconstructed skulls, 27 (54%) were estimated to be male, and 23 (46%) female, based on such criteria as general size and robusticity. Tentative sex attributions were also made on 67 partial or complete mandibles: 37 (55.2%) were categorized as male, and 30 (44.8%) as female. The demographic profile of 199-F1 is compared with the other four excavated features in Tables C.3 and C.4.

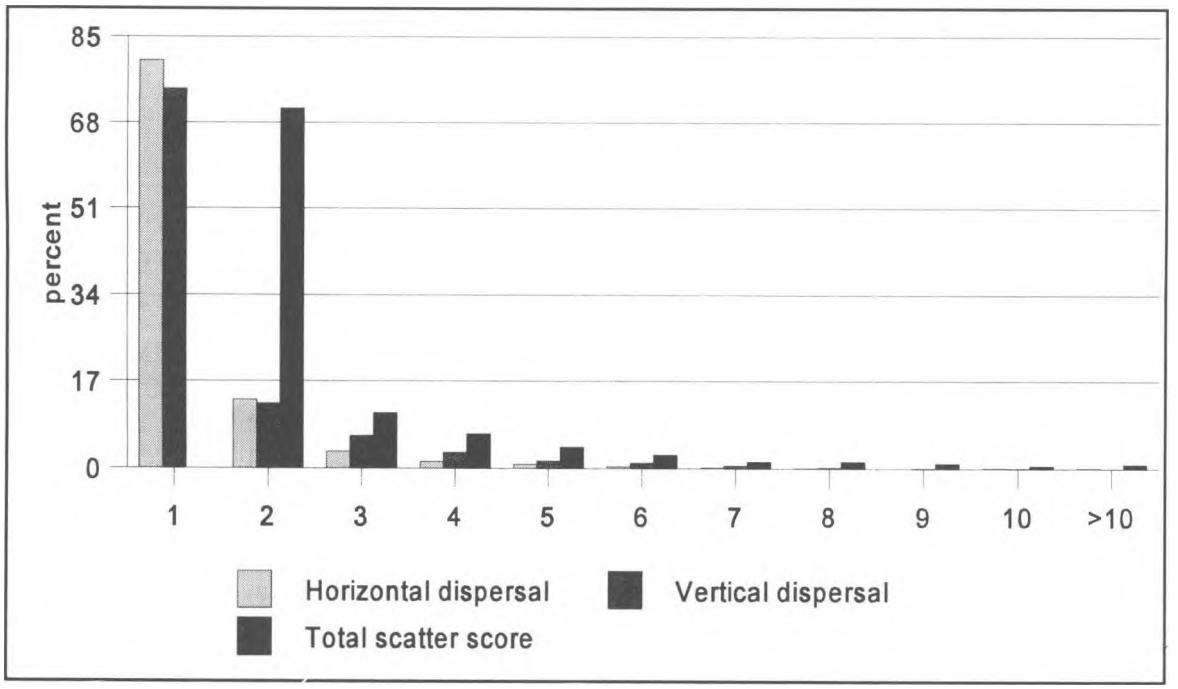

Figure 8.12 Dispersal scores of reconstructed elements, DgRw 199-F1.

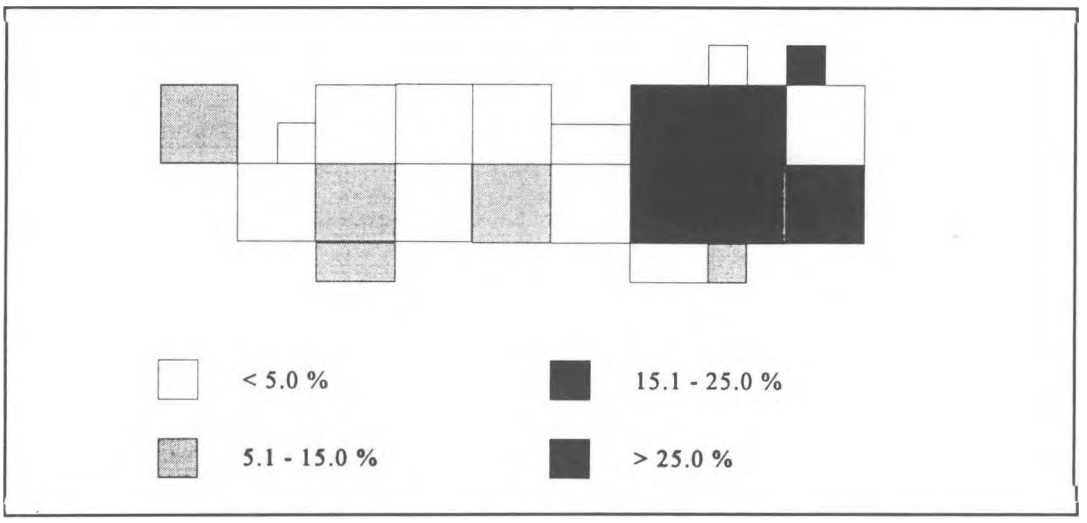

Figure 8.13 Horizontal distribution of subadult remains (% of unit total).

demographic profile of 199-F1 is compared with the other four excavated features in Tables C.3 and C.4.

Anomalies and Pathologies

Numerous anomalous and pathological conditions were observed in the skeletal material from 199-F1. Only the most significant are discussed below.

Degenerative joint disease is ubiquitous in the collection, but is not quantified here due to the difficulties encountered in identifying individual joints in such fragmented material. The impression given by viewing the remains, however, is one of higher prevalence and greater severity of osteoarthritic lesions than any of the other four excavated skeletal samples. Of particular interest are the distinctive lesions observed on seven right and eight left distal humeri, which exhibit hypertrophic bone deposits in the radial, coronoid, and/or olecranon fossae (illustrated in Skinner 1991: 64ff). While similar lesions in other skeletal collections have been attributed to severe degenerative arthritis (Ortner and Putschar 1981: 425), Skinner raises the possibility of a treponemal origin, suggest-

sals, 6 metatarsals, and 27 phalanges. Next in fracture frequency is the hand (n=6: 1 metacarpal, 5 phalanges), followed by the knee (n=3: 1 tibia, 2 fibulae), shoulder (n=2 clavicles), arm (1 humerus), and forearm (1 radius), and an unidentified long bone shaft.

The cranial fractures provide good evidence for direct interpersonal violence in the False Narrows bluffs population, which in at least five cases (*peri mortem* and incompletely healed fractures) may have led to the deaths of the affected individuals. Some or all of the rib fractures may also have resulted from interpersonal violence, although in these cases it is difficult to distinguish from accidental trauma such as would occur in a fall, or from a blow to the chest or back. The remainder of the skeletal fractures are probably the natural result of the indirect traumas and long-term stresses experienced in the course of a vigorous, active life. The clavicle and radius fractures, for example, are typical of injuries incurred in falls onto the shoulder or outstretched hand; wedge compression fractures of the vertebrae are a common sequella of heavy falls onto the feet or buttocks (Adams 1978); spondylolysis tends to develop in response to chronic heavy-loading stress to the lower back (Merbs 1989); fractures to lower cervical and upper thoracic spinous processes have been attributed to strenuous muscular exertion in shovelling or similar activities (Knüsel et al. 1996); and the ubiquitous ankle and foot injuries can be attributed no doubt to inadequately shod travel along our perilous rocky coastline.

Chronic stress to the vertebral column can result in injuries other than skeletal fracture, including subluxation of apophyseal facets and Schmorl's nodes on vertebral centra, both of which were observed in this assemblage. Remodelling of apophyseal facets indicative of subluxation was observed in 15 cervical and 18 thoracic vertebrae. In five cases, the altered joint space brought the spinous processes of adjacent vertebrae into contact, with the subsequent development of flat articular facets on their dorsal and/or ventral surfaces. Schmorl's nodes, resulting from the degeneration of the intervertebral disc, were observed in 3 cervical, 16 thoracic, and 8 lumbar vertebrae.

Only one example of chronic dislocation was found in the appendicular skeleton, involving a pedal distal interphalangeal joint. The distal articular surface of the middle phalanx is rough and pitted, and a new articulation with strongly lipped margins has formed on the distal plantar surface.

Numerous **developmental defects** of the skeleton and teeth were also observed in this collection. Axial defects include one definite and two possible instances of "block vertebrae", resulting from segmentation failure of the sclerotomes. The first example, from a very young, possibly newborn infant, involves the neural arches from two lower cervical vertebrae that are joined posteriorly near the spinous process. This is most likely a case of Klippel-Feil syndrome, Type II, which is inherited as an autosomal recessive trait, and is generally asymptomatic (Barnes 1994). The other possible examples of Type II block vertebrae are two pairs of thoracic vertebral arches joined from the articular facets to the spinous process; unfortunately these are incomplete specimens lacking centra, so one cannot eliminate trauma or other pathological conditions (e.g. DISH or ankylosing spondylitis) as diagnostic possibilities.

Six examples of vertebral border shifts were identified, two involving the thoraco-lumbar region (vertebrae intermediate morphologically between thoracic and lumbar), and four the lumbosacral region (one completely and three partially sacralized fifth lumbar vertebrae). One of the latter is an unusual tripartite fifth lumbar vertebra exhibiting both spondylolysis (see Table 8.6) and spina bifida (cleft neural arch). Two other cases of spina bifida were recorded, one a complete but narrow cleft in an adult axis vertebra, the other a cleft first sacral vertebra from a 6-7 year old child. The latter may be merely a case of delayed rather than failed union, but the articulating second sacral vertebra has already fused completely, so this possibility seems unlikely. Possible cases of delayed union of neural arch halves include seven thoracic and one first sacral vertebrae with deep midline notches on the superior margins of their neural arches.

Dental anomalies observed in the collection include one mesiodens (midline supernumerary tooth) in an child's maxilla, a notched permanent lateral incisor in a child's mandible, and two examples of mandibular supernumerary teeth, occurring in the premolar region of adult mandibles. One supernumerary has erupted lingual to and between the two right permanent premolars; the other is unerupted and located in a crypt between the two left permanent premolars.

Bilateral agenesis of the permanent central incisors was seen in four mandibles (two children, two adult females); in these cases the morphology of the developed lateral incisors is intermediate between a normal central and normal lateral incisor, and a diastema of variable size is present between them. Bilateral agenesis of the permanent central incisors was seen in four mandibles (two children, two adult females); in these cases the morphology of the developed lateral incisors is intermediate between a normal central and normal lateral incisor, and a diastema of variable size is present between them. Agenesis of the permanent third molar occurs unilaterally in three mandibles (all left sides), and bilaterally in one of the

Table 8.6 Skeletal fractures, DgRw 199-F1.

Element	Portion	Comment
Skull D	anterior R. parietal	healed depressed fracture; margins incomplete; inner table unaffected
Skull F	mid-frontal squama	healed depressed fracture; 20 x 14 mm; deep; inner table unaffected
Skull H	middle L. parietal	healed depressed fracture; 21 x 16 mm; well-defined; inner table unaffected
Skull U	posterior R. parietal	healed depressed fracture; 16 x 12 mm; shallow; inner table unaffected
Skull Z	L. frontal squama	healed depressed fracture; 12 x 10 mm; ill-defined; inner table unaffected
Skull Z	L. coronoid suture	healed depressed fracture; 27 x 20 mm; deep; inner table unaffected
Skull 7580S:1	R. superior occipital	*peri mortem* linear fracture, runs down to F. magnum and forward to R. orbit
Skull 7580S:4	R. parietal/temporal	*peri mortem* linear fracture, from parietal notch forward across middle of R. coronal suture
Skull 8085S:3	L. frontal squama	healed depressed fracture; 14 x 9 mm; ill-defined; inner table unaffected
Skull 10396	posterior R. parietal	healed depressed fracture; 25 x 20 mm; deep; inner table unaffected
Skull 34051	L. lambdoidal suture	healed depressed fracture; 25 mm; deep; inner table thinned and pitted
Skull 36656	anterior L. parietal	healing depressed fracture; 17 mm; perforation due to necrosis/ sequestration; exposed diploë thickened; spongy reactive bone on inner table
Skull 40563	L. frontal	healed depressed fracture; 27 x 10 mm; slight bulge on inner table
Skull 40563	anterior L. parietal	unhealed depressed fracture; 15 mm circle; 34 x 29mm inner table displaced inward; triangular area of hyper-vascularity surrounds lesion on inner and outer table
Skull 41110	R. frontal	healed depressed fracture, 26 x 20 mm; inner table unaffected
Skull 5295	R. frontal	healed depressed fracture; 6.5 mm diameter; inner table unaffected
Skull 1167	R. frontal	healed depressed fracture; 8 x 5 mm; shallow; inner table unaffected
Skull 53690	superior R. occipital	healed depressed fracture; 18 mm; shallow; inner table unaffected
Skull 29380	L. parietal	*peri mortem* penetrating wound; 11 x 6 mm; inner table curled inward
L. rib 10-11	middle/vertebral 1/3	healed fracture, dorsal displacement vertebral 1/3
R. rib	sternal 1/3	healed fracture with non-union of ends
R. rib	angle	healed fracture, slight inferior displacement
R. rib	sternal end	healed fracture
R. rib	sternal tip	healed fracture with non-union of ends
R. rib	shaft fragment	healing fracture with callus (juvenile)
R. rib	shaft fragment	healed fracture with slight angulation
R. rib	shaft fragment	healed fracture with non-union of ends
L. rib	shaft fragment	healing fracture with callus (juvenile)
R. rib	shaft fragment	healing fracture with callus
L. rib 11-12	shaft fragment	healed fracture
Rib (immature)	sternal end	healed fracture with non-union of ends
L. rib #1	complete	well-healed fracture of neck; slight distortion
R. rib	shaft fragment	healed fracture with slight angulation
R. rib	angle fragment	healed fracture with moderate displacement
rib	shaft fragment	healed fracture
cervical vert. #7	spinous process	healed fracture, spinous process deflected to left
thoracic vert. #2	spinous process	healed fracture, slight deformity near tip
thoracic vertebra	spinous process	healed fracture with lateral displacement to left
thoracic vertebra	inferior centrum	healed compression fracture, centrum collapsed
thoracic vertebra	inferior centrum	healed compression fracture, centrum collapsed
thoracic vertebra	centrum	healed compression fracture; wedge-shaped centrum

Table 8.6 Skeletal fractures, DgRw 199-F1 continued.

Element	Portion	Comment
thoracic vertebra	inferior centrum	healed compression fracture; wedge-shaped centrum
thoracic vertebra	centrum	healed compression fracture; anterior wedging
thoracic vertebra	centrum	healed compression fracture; anterior wedging
thoracic vertebra	centrum	healed compression fracture; anterior wedging
thoracic vertebra	centrum	healed compression fracture; anterior wedging
thoracic vertebra	centrum	healed compression fracture; anterior wedging
thoracic vertebra	centrum	healed compression fracture; anterior wedging
thoracic vertebra	centrum	healed compression fracture; anterior wedging
thoracic vertebra	centrum	healed compression fracture; anterior wedging
thoracic vertebra	L. sup. articular facet	healed fracture superomedial margin
thoracic vertebra	L. sup. articular facet	healed fracture superolateral margin
thoracic vertebra	R. sup. articular facet	healed fracture lateral margin
lumbar vertebra	R. inf. articular facet	healed fracture inferior tip, slight dorsal displacement
lumbar vertebra	centrum	healed compression fracture; moderate wedging
lumbar vertebra	centrum	healed compression fracture; moderate wedging
lumbar vertebra	centrum	healed compression fracture; centrum collapsed
lumbar vertebra	centrum	healed compression fracture; centrum collapsed
lumbar vertebra	centrum	healed compression fracture; centrum collapsed
lumbar vertebra	centrum	healed compression fracture; slight anterior wedging
lumbar vertebra 5	complete	complete bilateral spondylolysis
lumbar vertebra 5	complete	complete bilateral spondylolysis
lumbar vertebra 5	complete	tripartite: complete bilateral spondylolysis with *spina bifida* of inferior arch half
lumbar vertebra 5	inferior arch	complete bilateral spondylolysis
R. clavicle	lateral shaft	healed fracture, anterior displacement lateral end
L. clavicle	medial shaft	healed fracture; strong angular deformity
long bone	shaft fragment	partially healed fracture with callus formation
L. humerus	midshaft	partially healed oblique fracture, large callus, incompletely closed medullary canal; proximal shaft osteoporotic (pathological fracture?)
L. radius	distal shaft	healed fracture with remodelled callus and slight dorsal displacement of distal fragment
metacarpal 3	prox. articular surface	fracture to base of styloid and metacarpal 2 facet
prox. hand phalanx	prox. articular surface	healed fracture right margin
prox. hand phalanx	distal articular surface	healed crush fracture of central articular area
dist hand phalanx	prox. articular surface	healed crush fracture of articular facet
dist hand phalanx	prox. articular surface	healed crush fracture with severe osteoarthritis
dist hand phalanx	prox. articular surface	healed fracture, articular surface inferior margin
L. tibia	lateral condyle	healed compression fracture, dorsal-lateral margin
L. tibia	medial malleolus	healed avulsion fracture with non-union of malleolus
L. fibula	prox. articular surface	linear oblique fracture with secondary osteoarthritis
R. fibula	proximal shaft	fracture callus at broken end of shaft fragment
L. fibula	distal shaft	well-healed fracture, slight lateral displacement
R. fibula	distal articular surface	oblique linear fracture of articular surface
L. fibula	distal articular surface	oblique linear fracture of articular surface
L. calcaneus	anterior talar facet	healed crush fracture of medial margin of facet
L. cuboid	distal articular surface	crush fracture inferior margin 4th metatarsal facet
L. cuneiform #1	prox. articular surface	crush fracture of navicular facet
L. cuneiform #3	distal articular surface	crush fracture inferior margin 3rd metatarsal facet

Table 8.6 Skeletal fractures, DgRw 199-F1 continued.

Element	Portion	Comment
L. metatarsal #1	prox. articular surface	crush fracture superior margin 1st cuneiform facet
L. metatarsal #2	prox. articular surface	crush fracture superior lateral corner of facet
R. metatarsal #2	prox. articular surface	transverse linear fracture mid-facet
R. metatarsal #2	prox. articular surface	crush fracture superior-lateral corner of facet
L. metatarsal #3	prox. articular surface	crush fracture superior-medial corner of facet
metatarsal #2-5	prox. articular surface	crush fracture middle articular surface
prox. foot phalanx	prox. articular surface	crush fracture inferior lateral corner of facet
prox. foot phalanx	prox. articular surface	crush fracture inferior third of facet
prox. foot phalanx	prox. articular surface	healed fracture with secondary arthritic lipping
prox. foot phalanx	prox. articular surface	oblique linear fracture of facet
prox. foot phalanx	distal articular surface	crush fracture with severe secondary osteoarthritis
prox. foot phalanx	distal articular surface	crush fracture of proximal interphalangeal joint
prox. foot phalanx	distal articular surface	crush fracture of proximal interphalangeal joint
prox. foot phalanx	distal articular surface	crush fracture of proximal interphalangeal joint
prox. foot phalanx	distal articular surface	crush fracture of proximal interphalangeal joint
mid. foot phalanx	prox. articular surface	crush fracture inferior lateral corner facet
mid. foot phalanx	prox. articular surface	crush fracture
mid. foot phalanx	prox. articular surface	crush fracture inferior third of facet
mid. foot phalanx	prox. articular surface	transverse linear fracture of facet
dist. foot phalanx 1	prox. articular surface	crush fracture medial half facet
dist. foot phalanx 1	prox. articular surface	crush fracture medial half facet
dist. foot phalanx 1	prox. articular surface	transverse linear fracture with secondary osteoarthritis
dist. foot phalanx 1	prox. articular surface	crush fracture lateral half facet
dist. foot phalanx 1	prox. articular surface	comminuted crush fracture of entire articular surface
dist. foot phalanx 1	distal shaft	transverse fracture, lateral displacement of distal end
dist. foot phalanx	prox. articular surface	crush fracture
dist. foot phalanx	prox. articular surface	comminuted crush fracture with severe osteoarthritis
dist. foot phalanx	prox. articular surface	crush fracture
dist. foot phalanx	prox. articular surface	crush fracture with secondary osteoarthritis
dist. foot phalanx	prox. articular surface	crush fracture
dist. foot phalanx	prox. articular surface	crush fracture
dist. foot phalanx	prox. articular surface	transverse linear fracture
dist. foot phalanx	prox. articular surface	transverse linear fracture with secondary osteoarthritis

adult females with central incisor agenesis. Four additional partial mandibles exhibit third molar agenesis on one side (three right, one left). Dental reduction or agenesis is considerably less common in the maxillary teeth, with only three instances observed: agenesis of the left lateral incisor in an incomplete child's maxilla, a peg-shaped right third molar in a partial juvenile maxilla, and agenesis of the right third molar in an incomplete adult maxilla.

Developmental defects of the appendicular skeleton are limited to the hands and feet. The presence of anomalous accessory ossicles in the wrist region are inferred from the absence or reduction of the hamulus on two right hamates (*os hamulare basale* or *os hamuli proprium*), and absence of the styloid process (*os styloideum*) on six right and two left third metacarpals (O'Rahilly 1953). Abnormal shortening (*brachydactyly*) was observed in four metapodials: a right third and fourth metacarpal (possibly from the same hand), and a left and right fourth metatarsal (probably antimeres from the same skeleton). Finally, 12 fifth pedal digits exhibit fusion of the middle and distal phalanges. Although ankylosis secondary to trauma cannot be ruled out in the etiology of this variant, the fact that only fifth digits are affected, that only one of the 12 examples exhibits any overt evidence of trauma, along with the observation that ankylosis was

not observed in other unequivocal cases of trauma, argues against this interpretation.

Evidence of **cultural modification** is not common in the skeletal remains from this assemblage. Artificial cranial deformation is limited to one definite case (an adult female skull with mild bifrontal-occipital deformation) and two possible examples involving subadults: an infant with bilateral flattening and focal resorptive lesions on both frontal bosses, and a child's frontal bone exhibiting the median frontal ridge and flattened frontal bosses typical of the bifrontal mode of deformation. Similar lesions were observed in infant skulls from the Tsawwassen site, and were also attributed to deformation (Curtin 1990b).The introduction of artificial deformation is thought to have occurred sometime in the late Locarno or early Marpole periods of prehistory in this region (Beattie 1980), which would make the specimens from Gabriola among the earliest documented examples of the practice.

Cultural modification is more common in dental remains from 199-F1. Polish and/or attrition of the lingual surfaces of anterior teeth were observed in 15 mandibles and one maxilla (6 males, 6 females, 3 adults of indeterminate sex, and one child). Since tooth wear from masticatory function is normally confined to the occlusal/incisal surfaces, this pattern of lingual attrition is suggestive of non-masticatory tooth use, probably in some task-related function such as the processing of hides or fibres. Irregular patterns of occlusal attrition on the posterior teeth of seven mandibles and on the anterior teeth of three others provides corroboratory evidence of the frequent use of the teeth for task-related functions. One final example of dental modification was seen in an adult male mandible with a narrow, obliquely-oriented groove on the occlusal surface of the left first premolar. Similar grooves have been reported in the prehistoric skeletal samples from Prince Rupert Harbour (Cybulski 1974) and Tsawwassen (Curtin 1991a), where they were attributed to the processing of plant fibres or animal sinew.

There are many indications of **infectious disease** processes affecting the skeletal remains from 199-F1. In an earlier report on the small sample of human bones collected from this burial feature in 1987, Skinner (1991: 61-66) described pathological changes affecting 10 skeletal elements (a skull, 2 ulnae, 4 femora, a tibia, a fibula, and a rib) from a minimum of three individuals, which he attributed to treponemal infection. Although the infracranial lesions are suggestive but not diagnostic of this syndrome of diseases, the skull exhibits ectocranial lesions of the classic *caries sicca* sequence, including confluent clustered pits, focal superficial cavitations, circumvallate and serpiginous cavitations, and radial scars (Figure 8.14; Skinner 1991: Fig. 16-24) which are considered pathognomic of treponemal disease (Hackett 1976).

The larger assemblage of human skeletal material recovered in 1991 provides abundant additional evidence of infectious disease, and corroboration for Skinner's initial diagnosis. The osseous changes are most commonly manifested as periostosis, the deposition of hypertrophic new bone on periosteal surfaces, primarily but not exclusively affecting long bone diaphyses. The morphology of the periosteal deposits varies from small diffuse patches of spongy-textured fibre bone, to larger, localized fusiform swellings often with a lamellar structure, to more extensive sclerotic expansions involving large areas of the shaft and in severe cases substantially altering its shape. In at least one tibia, apposition along the anterior crest has resulted in the characteristic "sabre shin" appearance often associated with treponemal infection. In the more severely affected specimens, hypertrophic endosteal deposits may also be present either as small localized patches of spongy bone adhering to the endosteal surface or as an expansive mass of fine cancellous tissue occluding the medullary cavity. In a few, diagnostically significant cases, sharp-margined expanding cavitations are found in the hypertrophic periosteal new bone, apparent foci of gummatous inflammation. This combination of periosteal apposition and focal cavitation was considered by Hackett (1976: 93-97) to be a diagnostic criterion of "syphilis" (treponemal disease).

A total of 232 identifiable skeletal elements exhibit these osseous changes to some degree, in addition to 526 unidentified long bone shaft fragments from an undetermined number of skeletal elements (Table 8.7). A minimum of 17 individuals are affected, including at least 11 adults and 6 subadults (3 infants, 2 children, 1 adolescent). Figures 8.15 - 8.17 illustrate typical infectious lesions in a femur, humerus, and two fibulae. The distal two-thirds of the right femur (Figure 8.15a) appears swollen due to the presence of rugose periosteal new bone cloaking the shaft; in close-up (Figure 8.15b), it has a smoothly rippled appearance marked by vascular grooves, small clusters of pits, and small depressions or "dimples" that probably represent healed, remodelled gummatous lesions. An active lesion is present on the ventral-medial aspect of the proximal shaft (Figure 8.15c): a small irregular sharp-margined cavity surrounded by an oval area of reactive fibre bone and periostitis.

Table 8.7 Evidence of infectious disease, DgRw 199-F1.

Element	N	Periosteal Deposition	Endosteal Deposition*	Cavitatation	MNI	Adult	Sub Adult
skull	1	1	1	1	1	1	
zygoma	1	1	1		1	1	
mandible	1	1			1	1	
sternum	2	2			2	2	
clavicle	18	18	4		9	8	1
scapula	8	8		1	2	1	1
rib	28	28	4	1	3	1	2
humerus	22	22	3	3	11	11	
radius	7	7	2	1	4	3	1
ulna	13	13	2	1	4	3	1
carpal	1	1			1	1	
metacarpal	18	18	1		4	4	
phalanx	14	14	1		2	2	
innominate	3	3			1	1	
femur	17	17	4	5	7	6	1
tibia	25	25	2	1	10	5	5
fibula	26	26	9	5	5	5	
tarsal	3	3			1	1	
metatarsal	8	8	3		3	2	1
phalanx	6	6			1	1	
vertebrae	8	8			2	2	
sacrum	2	2			2	2	
long bone	526	526	89				
Total	**758**	**758**	**26**	**19**	**17**	**11**	**6**

* underestimates true frequency, since only observable in fragmented or radiographed specimens.

Similar but more extensive changes are apparent in the right humerus, shown in ventral (Figure 8.16a) and dorsal (Figure 8.16b) views. The distal shaft is grossly swollen and distorted, and pocked with superficial cavitations in various stages of healing. The more proximally-located lesions appear to be more recent than the distal ones, whose margins are collapsing and smoothing over as they begin to heal (Figure 8.16c). The two fibulae illustrated in Figure 8.17a exhibit varying degrees of periostosis on their distal shafts, including diffuse striated and pitted deposits (left) and localized fusiform swellings (right). The periostosis may occur alone (Figure 8.17b) or in conjunction with a focal cavitation (Figure 8.17c).

In younger subadults (infants and children) the diaphyseal periosteal reaction is typically expressed as a superficial sleeve of new bone which cloaks the original cortex (Figure 8.18); in some cases several distinct layers of periosteal bone are apparent. Unfortunately, poor preservation of immature long bone metaphyses precludes the identification of Wimberger's sign (symmetrical osteomyelitis of the proximal tibia), but one distal femoral epiphysis exhibits the distinctive jagged, erose margin of osteochondritis, another characteristic lesion of childhood treponematosis (Mansilla and Pijoan 1995).

In addition to these infracranial changes, dental remains from a six-year-old child exhibit morphological characteristics suggestive of congenital treponemal infection (Jacobi et al. 1992). The affected teeth are the two permanent mandibular first molars and the right permanent mandibular canine. The molars are severely hypoplastic, with rounded, bulbous cusp tips constricted at the base by a deep, irregularly pitted hypoplastic line that encircles the crown (Figure 8.19). The cusp tips appear crowded together towards the centre of the occlusal surface, which itself features many small irregular enamel globules (most apparent on the left molar), producing the "mulberry" appearance characteristic of Moon's molars. The canine (of which only the crown has yet formed) exhibits a deep, circumferential groove around the cusp tip, below which is a broad band of pitted hypoplastic enamel covering approximately one-third of the vertical di-

mension of the crown. The unerupted permanent mandibular incisors of this individual appear normal radiographically. Since the affected areas of the permanent molars and canine are those that are developing in the perinatal period, congenital transmission of the infectious agent seems indicated (Turner 1993). Similar dental stigmata are reported to occur in 30-45% of cases of congenital syphilis (Steinbock 1976: 106), although there is difference of opinion as to whether they can be considered pathognomic of that disease (Baker and Armelagos 1988; Hackett 1976).

Taken together, the neonatal dental lesions, the cranium with *caries sicca*, and the long bones with periostosis and focal cavitations all support a diagnosis of treponemal disease endemic in this population. There are four closely-related diseases or syndromes subsumed under the term treponematoses: pinta, yaws, treponarid (also known as bejel or endemic syphilis), and venereal syphilis; each results from infection with a variety or species of the *Treponema* spirochete, but only the last three are known to affect the skeleton (Ortner and Putschar 1981: 180). Yaws and treponarid are typically contracted in childhood, and most commonly transmitted by body contact or by the use of common eating utensils; syphilis usually affects older adolescents and adults, and is transmitted primarily through sexual contact. Unfortunately, the osseous lesions of yaws, treponarid, and venereal syphilis are morphologically indistinguishable, although some attempts have been made to differentiate between the three entities on the basis of their patterns of skeletal involvement (Steinbock 1976; Ortner and Putschar 1981; Rothschild and Heathcote 1993; Rothschild and Rothschild 1994, 1995; Hershkovitz et al. 1994).

The demonstration of congenital infection has long been considered essential to the diagnosis of venereal syphilis in skeletal remains (e.g., Baker and Armelagos 1988; Powell 1994; Cook 1994), since transplacental infection of the fetus, while *theoretically* possible in all three syndromes, can only occur if the maternal infection is in the secondary phase during pregnancy, and with yaws and treponarid, which are normally contracted in childhood, this stage is never found in pregnant women, at least in modern cases (Grmek 1994). Baker and Armelagos (1988: 705), for example, consider the occurrence osteochondritis and the dental stigmata as pathognomic of venereal syphilis. At 199-F1, therefore, the association of bone lesions pathognomic of treponemal disease with dental lesions indicative of congenital infection suggests that the specific treponemal infection afflicting the population was venereal syphilis. The high frequency of periostitis in arm bones at 199-F1 is also consistent with a diagnosis of venereal syphilis, since these bones are rarely affected by other infectious diseases (Steinbock 1976: 112; Rose and Hartnady 1991: 125).

Other diseases affecting the skeleton were considered in the differential diagnosis of the F1 infectious lesions, including neoplasm, trauma, pyogenic osteomyelitis, leprosy, Paget's disease, tuberculosis, and chronic leg ulcer but none of these were consistent with the observed skeletal manifestations.

Mortuary Practices

Despite the confounding effects of post depositional taphonomic processes on the integrity of the deposits at 199-F1, some clear patterns of mortuary behaviour can be discerned. The artifact associations indicate that at least some of the bodies interred here were people of wealth and prestige in their community. The high incidence of cranial fractures, and the tentative evidence of post mortem mutilation suggest that some may have died violently. Others may have succumbed to infectious disease. Many of the bodies were thoroughly cremated, and all may have been exposed to fire at least minimally during the mortuary ritual. Some of the crania with pathological or traumatic lesions are largely unburnt except for localized areas of charring in the vicinity of the lesions, suggesting an intimate association between burning ritual and cause or manner of death.

Burning patterns indicate that the bodies were cremated in the flesh, and the presence of cutmarks near major joints suggests that some were at least partially dismembered prior to cremation. There are no indications that the cremation took place inside the burial feature: no fire-altered rocks, no ash layers, no dense concentrations of charcoal. Although none of the skeletal remains was found articulated in anatomical position (further support for *post mortem* dismemberment), the relatively low dispersal rate of fragments from the same bone, and of elements from the same individual (where discernible) suggest that the bodies were processed individually, instead of part of a mass cremation. Food offerings consisting primarily of fish and shellfish were left for the dead at the time of deposition and perhaps periodically afterwards.

There are some suggestions that skeletal elements, particularly near the entrance passage, may have been cleared aside and sorted prior to subsequent interments, and that the remains of subadults were preferentially placed in the east chamber of the cave. Radiocarbon dates indicate that this feature was reused over a long span of time, perhaps a thousand years or more, and that the likelihood of cremation, or the intensity and thoroughness of cremation, or both, diminished during the later history of the burial cave.

Figure 8.14 ***Caries sicca*** **lesions on cranium: (A) frontal view; (B) vertical view.**

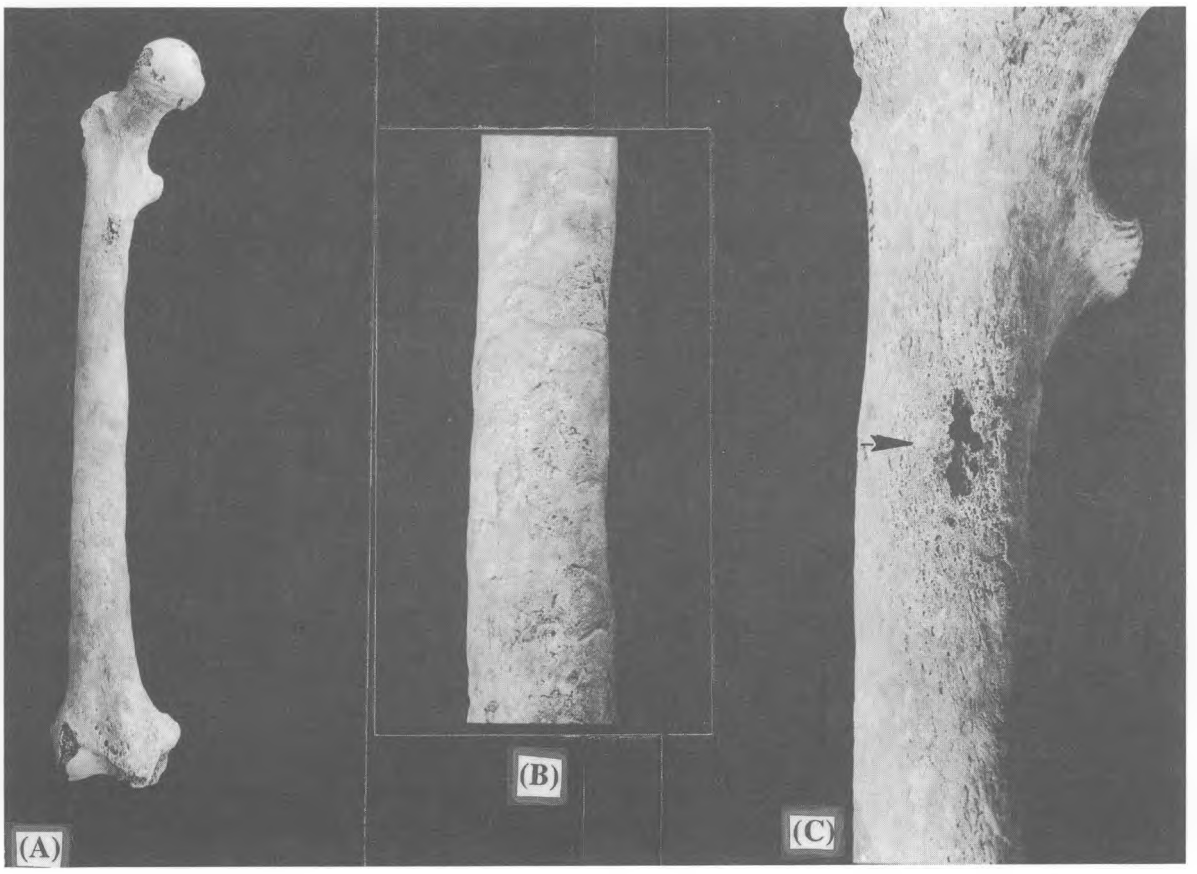

Figure 8.15 Periosteal lesions on femur: (A) ventral view: (B) close-up of midshaft periostosis: (C) focal cavitation on proximal ventral shaft.

Figure 8.16 Periosteal lesions on humerus: (A) ventral; (B) dorsal; (C) close-up.

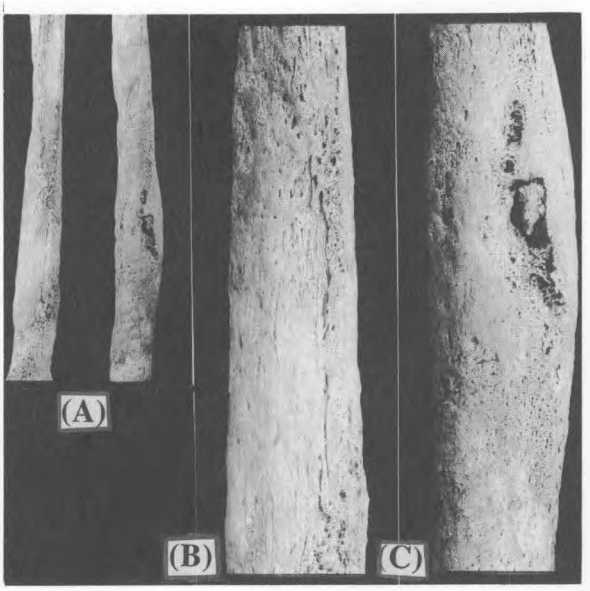

Figure 8.17 Periosteal lesions on fibulae: (A) two distal shafts; (B) periostosis: (C) focal cavitation.

Figure 8.18 Child's femur with sleeve of periosteal new bone.

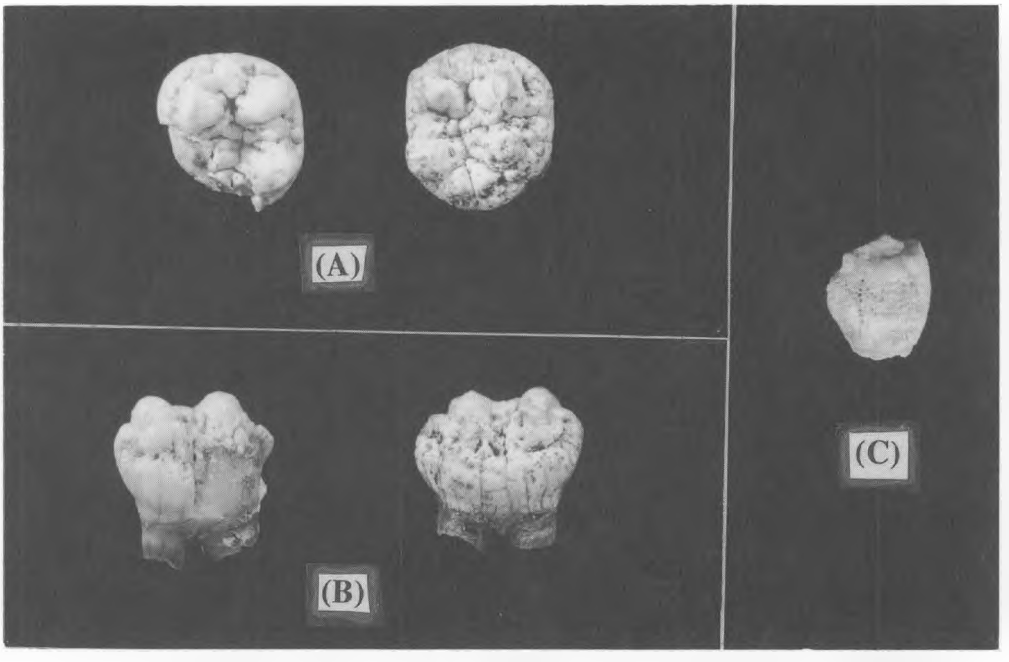

Figure 8.19 Dental stigmata of congenital treponemal disease: mandibular first molars: (A) occlusal; (B) buccal; (C) right canine crown, labial view.